

Challenges in the aviation system caused by the emergence of delivery drones

Zsolt SÁNDOR

University of Tokaj
Eötvös Út 7. Sárospatak, H-3950, Hungary
*e-mail: Zsolt.sandor1@gmail.com

Submitted: 11/01/2023 Accepted: 27/01/2023 Published online: 06/02/2023

Abstract: Using unmanned aerial systems is spreading in several industry sectors. New and previously not seen demands are evolving in the service provider sector. Due to the continuous technological development in the aviation and drone segment, this equipment can fulfil delivery tasks beyond the previously elaborated data collection operations. The professionals should present the possible and potential adverse effects of drones caused by the emergence and large-scale spread of the devices beyond the demonstrated benefits and advantages.

Keywords: *delivery drone; drone; UAV; UAS; drone law; drone operations*

I. INTRODUCTION

The market connected to unmanned aerial vehicles (UAVs or simply drones) is a unique industry area with continuously growing capitalisation whose value has reached 127 billion US dollars, according to the estimations in 2021 [1]. Furthermore, the global scale of the market - limited only to the equipment - will grow from 14 billion to 43 billion US dollars in 6 years between 2018 and 2024. Thus it is expected that more than 100 thousand new jobs will be forming worldwide [2].

Previously, the main direction unmanned aerial vehicles' development was focuning on data collection and monitoring. Nowadays, technological developments are focusing on active interventions. New solutions are supporting the creation of novel use-cases of the UASs that will help to mitigate traffic congestion and connect other adverse effects caused by road transport through the active usage of the UAVs [3].

New technology solutions can satisfy the increasing demand for faster transport needs. Its organic part is the use of unmanned aerial systems, which are applied for special transport operations. These solutions are available even today at those locations where the road infrastructure is not available, or its quality does not support effective road transport (e.g. for the transport of medicines, vaccinations, and medical equipment) [4], [5], [6], [10].

The global market of the logistics sector, which is supported by unmanned aerial vehicles, is continuously growing. According to the forecasts, it will grow from its 5.3 billion US dollars value (2019) to 11 billion US dollars by its value by 2026 [7].

The topic of this article was given by the drones appearing in the commercial transport of goods. Their applications are raising several questions (so-called challenges) beyond the potential benefits, and these questions should be analysed from the viewpoint of air transport, environment protection and logistics. These challenges should be managed. Otherwise, the use of drones will be impossible, or the application of drones will affect the other players of air transport adversely, and they can deform commercial services.

In the last few years, the big international courier express and delivery companies have conducted intensive research to find innovative freight delivery solutions for the last-mile logistics of goods. In addition, Amazon, DHL and Google have devoted significant resources to find solutions for the usage of UAVs in future air transportation, thus providing a breakthrough in the sector.

This topic should be revealed because innovations have high priority in the last-mile transport while the parcel is transported from the warehouse to the consumer. This process is the most time-consuming, expensive, and polluting phase of the supply chain (explicitly calculated for a delivered parcel). Approximately 50% of the total cost is last-mile

delivery. Therefore, the market of package delivery executed by unmanned aerial vehicles is on the verge of a real revolution. Based on the forecasts, the global market of drone delivery services will reach 7.4 billion US dollars by 2027 with an annual 41.8% growth rate [8]. Other analyses are calculating over 50% annual growth rate and based on them, the capitalisation of the global market will reach 31 billion US dollars by 2028 [9].

Developments are made by international freight transport companies with road transport dominations and manufacturer companies with significant aviation experience [8]. Companies expect that due to the developments, UAV-executed freight delivery will become faster, greener, and much more environmentally friendly than conventional road transport.

With the developments, special applications can be used to support electricity or even hydrogen-based power of UAVs in the future. Thus it is possible that UAVs will not emit pollutants, and they can use the three dimensions of the space during the operations, so the ground-based traffic congestion will not affect their progress. A further advantage of delivery drones is that they can easily and quickly prepare for the flight (ready to fly). Loads can be easily inserted, batteries can be changed quickly (even under a few seconds), and the launch can be done seamlessly [31].

II. CHALLENGES

Innovations connected to delivery drones present only advantages in most cases. They emphasise that the application of this equipment positively contributes to environmental protection. Thus their usage is green and environmentally friendly, providing the elaboration of quick and reliable freight services. However, it can cause a false idea in people with less comprehensive industrial knowledge. Beyond the positive effects, this solution also has negatives. Technical, legal and regulatory challenges that arise with their use are not usually discussed. The more such services appear, the more significant these challenges will be, because drones executing freight transport activity in very low-level airspace significantly influence the operation of the aviation sector (even in the vicinity of airports and heliports). Beyond the operational issues, several demands are emerging concerning manufacturing and operation that needs a particular environment, which may overwrite the presumed advantages.

In this article, the author points out with the analysis of multiple factors that further innovations and attitude formation are needed for the rentability and widespread of UAV-based freight delivery and to conduct safe operations. Technology, legal, regulatory, sociology and psychical factors can be

identified as challenges. The author is analysing the challenges according to the following factors:

- Infrastructural challenges (air and ground equipment, components, life cycle).
- Energy-related challenges (source, cost and use of electrical energy).
- Demand and supply challenges (social attitude, solvent demand and social needs for these services).
- Legal challenges (possibility of use).
- Limitations due to physical accessibility.
- Effects on aviation players (restrictive effects on conventional aviation players, or the contrary, limitations caused by conventional aviation).

In order to better understand the individual factors, the author illustrates the effects of the limiting factors with the help of numerous application and calculation examples.

1. Infrastructural challenges

The infrastructure of UASs can be divided into the following parts:

- Unmanned aerial vehicle(s) > UAV: This is the freight transport drone. It executes the delivery task between the warehouse and the destination.
- Primary infrastructure: the set of all equipment and services needed to perform the flight operation directly. It consists of the followings:
 - Ground-based infrastructure: Service locations and the equipment and services used there (take-off and landing sites, where appropriate, the launch and recovery equipment, equipment required for operation preparation – equipment for charging batteries, etc.).
 - Airside base infrastructure: The set of equipment and services necessary for the operation of the air transport system (communication systems, airspace, tools for navigation, etc.).
 - Operational management base infrastructure: The management systems and components which are necessary for delivering goods and the delivery service (staff and the operational control centre).
- Secondary infrastructure: tools for servicing and maintaining the UAVs, maintenance base, educational facilities, simulators, etc.

A. Challenges by the unmanned aerial systems

The industrial sector of unmanned aerial systems has been significantly developed in the last decade. However, new technologies have arisen to solve the unconquerable problems in the past, limiting the spread and evolution of delivery drones. Nowadays, the most current and researched topic is finding answers for the most critical safety and security issues of drone flights and operations. These answers are significant in the case of UAV-based delivery

services. Flight operations are executed in BVLOS mode (beyond the visual line of sight) and fully autonomous due to the complexity of the operations and the great size of the covered area by the service. It requires the availability of advanced onboard electronic systems with high-level automation. This allows the execution of the missions fully automated between the take-off point and the destination without any human intervention by identifying all risks, hazards and barriers, thus supporting the execution of the necessary safety measures if needed.

The biggest challenge is the capacity limits of the applied UAVs from the operational point of view. They are limiting the maximum size and mass of the deliverable package and the maximum range of the service. In all cases, the service is performed with a well-defined drone fleet with precisely defined performance parameters. The followings are the most critical factors for the planning of the service (planning the maximum utilisation of devices):

- maximum range of the UAV with one single charging of the applied battery (maximum flying time),
- maximum size and mass of the deliverable package,
- the time necessary for the delivery at the destination,
- the time necessary for the re-deployment of the UAV after a mission when it comes back (time to recharge or change the battery and insert the new package),
- the possibility of a round trip (during the delivery, the device picks up another package and delivers it before returning to the warehouse),
- the possibility of delivering multiple packages to different addresses simultaneously.

Nowadays, the UAVs under design and construction can deliver and return only, so in case of an operation, the transport utilization can be a maximum of 50% on a time basis (see the application examples in the next chapter). The delivery and the re-deployment processes after the return need time, which further decreases the utilization. Thus, even in the best case, effective package delivery takes place in a maximum of 40-45% of the time spent in operation.

The determination of the active service period depends on the business policy, the length of the daylight and the weather. Delivery can be conducted only in daylight during favourable weather conditions from the viewpoint of operation when the recipient can receive the package. Otherwise, the receipt cannot be fulfilled. These conditions further limit the utilization of the service because favourable operational conditions are only available

occasionally during the year (e.g. all day between 8. AM. and 10 PM.).

Currently, drones can limitedly take part in freight transport. UAVs can transport parcels with a maximum of 1-2 kg weight, and their dimensions cannot exceed the dimension of a small shoebox. There are UAVs with more significant transport capacities (5-10 kg or even 20-30 kg). However, their design does not allow retail freight transport (they are fixed-wind UAVs instead of the multicopter design). The range of the UAVs depends on the maximum horizontal operational speed, the battery capacity and the weight of the transported load. Generally, it can be stated that a UAV with a multicopter design can fly for 15-20 minutes with the specified maximum load with one fully charged battery [11], [15].

Contrasting drone freight transport with road transport, it can be seen that drone delivery is much significantly dependent to the weather than road transport, and it has much lower utilisation if a single UAV is examined.

Further aspects are the prime and operational costs of the UASs. There may be one or more orders of magnitude differences between the prime cost in the case of a drone and a truck (even in the case of an electric-powered road truck, which cost equals 5-20 drones). In contrast with the costs, the capacity of the road truck is higher by one or more orders of magnitude. Thus its profitability and transport capacity are higher. From the viewpoint of operational costs, there may be significant differences. In the case of UASs, the following must be taken into account: cost of the electricity for the charging, maintenance costs, costs of the installation and operations of the mission control centre, costs of the supervisory staff, administration costs, insurance fees, costs of the continuous operation of the aviation safety and compliance monitoring solutions, system usage fees, etc. Because the UAV cannot deliver a considerable amount of goods, thus the higher operational costs are divided between a few parcels, resulting in high transport costs.

An example of the productivity of a UAV-based delivery service:

Delivery is carried out between 8 AM and 8 PM every day. Supposing that a UAV can deliver 1,5 parcels hourly on average on the operational territory (15-15 minutes flying to and from the destination, 5-5 minutes are the delivery and the re-deployment time), thus 18 parcels can be delivered within 12 hours by a single UAV, while its flying time is 8 hours. However, if the speed is increased and the turnaround time is decreased, and 24 parcels can be delivered within 12 hours, more is needed because a single truck can deliver this amount of goods within a few hours. Moreover, the UAV is not carrying and parcel during the back trip. Thus the capacity

utilisation is maximum 50% - theoretically – counted for the serviceable timebase.

From the viewpoint of this analysis, it is worth considering additional items from a technical point of view. First, the effects of the aircraft's production and the components' life cycle on the environment must be considered.

The fuselage, containment and engines resist environmental factors (weather, mechanical strains, etc.). Propeller blades should be exchanged periodically or in case they get damaged. Propellers are typically made with composites that can be easily and quickly manufactured and changed. When they become waste, recycling and waste management should be solved. From an environmental point of view, the most sensitive component is the battery. They must be charged after all operations, or a fully charged item should be placed into the UAV during the re-deployment processes. Charging is generally taken place separately from the UAV. The battery life cycles rapidly deteriorate, and manufacturers guarantee only a few hundred cycles. When the battery reaches the given cycle value, it cannot be safely used for the missions. Therefore, operators should provide that batteries are disposed of as waste. These obligations induce that drone delivery services may generate a significant amount of waste. The operators should manage them appropriately and professionally because this waste cannot be disposed of as communal waste.

For instance, the previously illustrated calculation can be used, supplemented with the information that the manufacturer determined a 500 cycle usage limitation. If the UAV completes 18 missions per day, after each 28 working days, one battery should be replaced by a new one due to deterioration. In the concrete situation, the operation is much more complex. Supposing a continuous operation, a single UAV uses more batteries according to the charging time. Generally, the fully charged status can be reached by 1-2 hours of charging time – with conventional, not fast charging. In the example, a single UAV uses four batteries, and all of them are available. Therefore, four waste batteries will be generated based on the parameters after 2000 mission. Count the average: one battery every month per a single UAV. The current calculation is connected to the currently available technology. It should be considered that in the case of fast charging, the deterioration can emerge sooner, at a lower cycle requiring oftener battery replacement.

When the drone delivery service will widespread and more delivery drones are used, thus thousands of batteries (thousands of tonnes) will appear as waste. Their safe disposal or reuse must be ensured.

B. Challenges by the primary and the secondary infrastructure

In order to operate the service, logistic centres (warehouses) are required from the UAVs can start the missions. Moreover, operation control centres are also needed, where service control and supervision are fulfilled. Therefore, while one operation control centre may be enough, more logistic centres (warehouses) should be installed according to the range of the applied UAVs, the covered territory by the delivery service, and the number of applied UAVs.

According to this, building one logistic centre (warehouse) in a region is not enough because the proper fulfilment of the service will need more. It will increase the investment and operation costs (more buildings should be built, more staff is needed, and operational costs are getting higher and higher. Thus, the fixed costs connected to the service are also increasing). It will have a significant effect on the specific costs. The infrastructure building costs are higher than the investment and operational costs of the UAVs, and this increase may even be several orders of magnitude. When the facilities are used for combined transport services (road and air), road-based freight transport may cross-finance the drone delivery service, decreasing the specific costs of the combined delivery service.

From environmental protection viewpoint, the adverse effects can be identified because the previously used economies of scale aspects are deteriorating. More buildings need much more energy, and if the source is not renewable, it may significantly increase the environmental load.

Moreover, the storage capacity is limited, and it needs more frequent freight transport due to the numerous but smaller warehouses. Therefore, it will increase the road-based freight transport needs. It is fulfilled by big, conventional, fossil-based trucks because electric-powered trucks are only limitedly available.

2. Energy-related challenges

In order to meet the environmental aims, the energy needed for the operation of the UAVs should be produced with the help of green resources, and its costs should be competitive and affordable. In the case of electric-powered vehicles, electricity is generated by renewable sources. In the case of non-electric powered vehicles (e.g. hydrogen-powered), the energy source should provide green and renewable conditions [30].

When the power energy source comes from non-renewable and non-green sources, then the drone delivery service cannot be considered an environmentally friendly transport solution, despite no pollutant emission at the location of the service.

There are numerous efforts to use electricity from green sources or green energy resources for innovative solutions, but the accessibility to these is limited. A solution could be installing renewable power plants (solar power plants or wind turbines) by the operators to cover the energy demand of the service. Energy demands arose in the following areas connected to the UAV-based delivery services:

- Direct energy needs of the UAVs – continuous charging of the batteries have significant energy demand.
- Energy required for primary and secondary infrastructures (direct energy demand of logistics centres, operation control centres).

The price of 1 kWh of electricity and the purchase possibilities of operators should be considered when calculating the energy needs. When the company is interested in using green energy from renewable sources, it is ready to pay higher fees for such electricity. The source and the electricity production are irrelevant if the main goal is cost reduction and the cheapest operation. The higher power costs will affect the service fees. Thus the costs will be paid by the customers.

From environmental protection and energetic viewpoint, the emergence and widespread of hydrogen-powered UAVs in the future can be a significant improvement possibility. However, green hydrogen production has to be developed for this advance, and safe containment and transport technology solutions must be elaborated for the onboard hydrogen. Moreover, the energy density of hydrogen is much higher than conventional batteries. Thus hydrogen-based technology can provide more flexibility for drone delivery services in the future. Further solutions are also the scope of research like the autonomous docking technology for battery replacement or charging, the laser-beam-based in-flight recharging and the combination of hybrid operation (combination of fuel cells, solar panels and super condensers) [11].

The currently applied and available lithium-ion batteries are limiting the spread of drone delivery services because their capacity does not allow long-distance flights. Technology developments are continuous, and battery capacities are expected to double by around 2025 compared to the capacities of the early 2020s years. However, the new capacities are lagging behind the possibilities provided by internal combustion engines. It is why drone delivery cannot be an efficient and competitive alternative to road delivery [12].

3. Demand and supply-related challenges

Drone delivery services are still evolving, and only a few parcel delivery companies have started the service in the retail sector as an experimental and pilot project. Accordingly, this service is at the

beginning of the Garter hyper cycle where research and development and early-stage retail solutions are found [13], [16], [17].

Several factors are influencing the demand for this service. Such as the fees, the real accessibility to the delivery (physical access – see next chapter), quantity and weight of the transportable goods, speed of the transport and the sensibility of the society to the innovations [32].

During the early stages of innovation, when its price is high (due to the need to cover innovation costs), it will be used by interested people eager to know the technology. Thus the demand will be low. With the evolving of the lifecycle and the growing accessibility of the service, the price will consolidate. However, the high complexity of the technology, high investment and operational costs and low capacity utilisation result that the fees of the drone delivery service will be much higher than road transport. In order to provide the continuous operation of the service, complex and expensive solutions have to be ensured at all times compared to road freight transport: safety management, compliance monitoring system, maintenance, operation control centre, detailed administration, unique and redundant communication systems, aviation-related systems, trained staff, training, etc. The extra fast delivery may increase the transport needs. It can be improved by increasing the service coverage from the supply side. However, this solution has a significant cost increase due to the need to install more logistics centres with more density.

Based on the available information, Amazon offers one delivery by a UAV for 63 USD [14]. This amount is approximately twentyfold of the road freight transport. The question arises whether the extra cost is commensurable with the advantage of the 30-60 minutes delivery, considering the maximum 2.5 kg limit of the parcel to be delivered.

4. Limitations due to physical accessibility

Delivery drones applied in the retail sector as pilot solutions can fulfil delivery operations only over significantly limited territories. Warehouses and destinations must be in appropriate proximity to each other, moreover the destination must be appropriate for the delivery made by UAVs. At the destination, over the delivery spot, the UAV lowers the parcel on a rope, or drops it, thus the location must be suitable for placing of the parcel by air. It is not realisable in dense downtown environment, in the surroundings of multi-storey apartment houses. Thus, the drone delivery service is limited to those locations, where the parcel placing can be safely conducted, like in the suburban, garden city houses.

Locations affected by drone delivery services can be found in complex airspace environments.

Complex airspaces may limit the accessibility to the service and the execution of the service because territories of half cities can fall under a No Drone Zone or in controlled airspace. Integrating the transport of UAVs into the conventional air traffic management system could be a solution that will be realisable with the emergence of UTM systems.

5. Legal challenges

Due to their nature, drone delivery operations can be executed in autonomous mode in BVLOS operations. Control, monitoring and surveillance of the UAVs are made from an operation control centre. Autonomous operations mean that during the execution of the mission, the remote pilot cannot intervene in the flight. Except the application of emergency procedures [18], [19]. The service can be provided only with autonomous operations because remote pilots can not control each UAV one by one during the fulfilment of the delivery. This nature necessitates further aviation safety requirements because safe operations must be ensured in all situations, even if unforeseeable obstacles, difficulties or malfunctions appear. Autonomous systems can identify and avoid static and moving obstacles (humans, animals, other drones or aircraft, cars, etc.) in the flight path without human interventions like self-driving vehicles. These operations can be performed only in the specific or certified category according to the EU regulations [18], [19]. These categories require that the operator has adequate operational authorisation issued by the competent authority. To gain this authorisation, the operator should comply with several technical, legal and operational requirements. During the operation of the service, the operator continuously has to prove the satisfaction of the safety requirement at the highest level. This over-regulation may limit the spread of drone delivery services in Europe.

6. Effects of drone delivery on the conventional player of the aviation

UAVs used for drone delivery use the same airspace as conventional aircraft but much lower. Conventional aircraft and UAVs can be separated because drones use airspace 50-150 meters above the ground, and other aircraft use much higher airspaces. However, there are situations when conventional aircraft use this low-level airspace, like in case of take-off and landing in the vicinity of airports or heliports and in case of special missions. Common airspace usage can result in conflict situations, near-bys and even collisions [25], [26], [27], [28], [29]. These risks are increasing with the growth of the number of applied UAVs. Implementing strategic mitigation measures can manage risks, but these measures cannot fully solve the potential risks independently that originated the common and joint airspace usage. The remaining risks originating from

the operation of UAVs can be mitigated by using tactical and operative risk mitigation measurements [19]. Although risks cannot be eliminated, they can be lowered to a commonly accepted level.

Due to the emerging conflicts, a drone delivery service can be operated only with several restricting provisions in a metropolitan area in case of a complex airspace structure. These restrictions will temporarily or permanently limit access to this service from a spatial aspect.

By the analysis of the airspace over Budapest, it can be stated that the No Drone Zones and the national flight limiting regulations permanently exclude 60 km² from the access of the service in Budapest. This permanently excluded area is 11% of the city, and the rest 89% may be the subject of temporary restrictions regularly.

7. Positive and negative effects of the service – summary of the main factors

Main issues and contributions are summarized in Table 1.

Table 1. Main issues and contributions

Positives	Negatives
<ul style="list-style-type: none"> - New service areas are evolving; - New technology solutions are developed; - A new mode of freight transport is applied; - The third dimension can be used for the transport of freight; - Transport is getting faster; - Inaccessible areas become accessible by this mean of transport. 	<ul style="list-style-type: none"> - Limited accessibility to the service in certain areas; - Detailed regulation is needed; - Difficulties in the integration of conventional air traffic management; - Limited transport capacity (mass and range); - Not obvious savings in the operational costs; - Additional load on the environment.

III. CURRENTLY AVAILABLE BEST PRACTISES

1. Retail drone delivery services

Delivery by UAV is the most promising application of drones because they can avoid congestion, and transported goods can be delivered on the optimal and shorter flight path, so the transport needs less time than road transport. Several companies offer this service on limited territories even though this freight transport technology is in the experimental and early application phase.

Amazon Prime Air service got authorisation from the American Federal Aviation Authority in the summer of 2022. Based on the authorisation, Amazon can execute BVLOS delivery operations. Service is suited for the transport of limited goods in limited territories. It is available in Lockeford, California State, at locations in the 15 miles vicinity of the warehouse. The weight of goods is limited to 5 pounds. The covered area is approximately 2000 km² [14]. According to the promises, the company can deliver the ordered parcels in one hour.

Beyond Amazon, DHL, Google, Mercedes-Benz and UPS are continuously conducting research and development activities to use UAVs in city logistics [20].

2. Non-commercial drone delivery solutions

Beyond the retail drone delivery services, there are special and unique UAV-based freight transport solutions with real added value. These services are used for non-commercial transport services at locations where road transport is not available due to its insufficiency. A state-of-the-art example of this solution is the operation when UAVs are used to transport medical equipment, life-saver medicines, vaccinations or other medical and biological samples in the countries of the third world at out-of-the-way locations. Fix-wing UAVs execute these operations because the delivery distances are generally longer than 50-100 km. Therefore operations are performed autonomously in BVLOS operations. This transport method is commonly used in the countries of the third world, and some companies are specialised in this.

Zipline Company executes these kinds of operations in Ghana and Ruanda in Africa, in Japan and in the United States of America. Fixed-wing UAV are deployed by a launcher and over the destination the parcel which is equipped with reusable parachute is dropped out from the UAV. After the drop, the UAV returns to the centre, where it is caught by a special net-based structure. Thus the physical operation infrastructure can be installed on the smallest area. Otherwise runway should be necessary for the operations. One centre can cover 22500 square km and one centre can control 20 UAVs simultaneously. UAVs have 160 km range, their cruising speed is 110 km/h and they can transport maximum 1.8 kg parcels [21], [22].

The solution of the Swedish EverDrone company is exemplary. It transports automated external defibrillators and other life-saver medical equipment by autonomously operated UAVs in BVLOS at those locations where they are needed in rural environments. Then, over the destination, the UAV lowers the life-saver equipment by rope, which allows the reanimation or the medical treatment

before the arrival of the ambulance, thus increasing the life expectations of the patient [23], [24].

IV. PARTICIPANTS OF THE DRONE DELIVERY SERVICE

The following list contains the main participants of the service, with the major information:

- **Client** > the customer, who would like to buy the product with drone delivery.
- **(Web)shop** > who sells the products and stores in warehouse, from the drone can be launched for the delivery.
- **Drone delivery service providers** > who provide the delivery service and operate the drones between the warehouses and the destinations (with the service operation control centre(s)).
- **Maintenance service providers** > who provide maintenance services for the drones.
- **Network operators** > who provide the data transmission network between the drone and the operation control centres.
- **Authorities** > who provide the oversights and other compulsories in order to fulfil a safe drone operation.
- **System integrators** > who provide integration between the different information systems. It is important to operate the service, because it is fully automated and flight are conducted autonomously.

V. SUMMARY

Based on the presented challenges, it can be stated that the large-scale appearance of drone delivery services in retail will generate environmental protection, transport organisational, air transport related and several other problems. Moreover, they may cause more oversized loads globally than the new services' benefits. The benefit is the acceleration of the delivery, but they have further demand-generating effects, which accelerate and increase the challenges.

During the elaboration of UAV-based delivery service, the operator should plan who, when and how and for what purposes will use it. There are several application areas where these kinds of services have significant importance and where they can offer real added value. These services are the following:

- Emergency transport of medicines, medical and life-saving equipment, vaccinations, biological and blood samples, etc., at locations where the road infrastructure is not available or the quality of the infrastructure does not offer the appropriate road transport.

- Transport of biological samples and human organs between hospitals and laboratories if air transport provides more efficacious (faster and safer) transport than road transport.
- Transport of equipment and materials used by emergency, law enforcement, search and rescue services (e.g. bomb detection and deactivation devices, removal of dangerous materials, search for missing people, etc.).

These applications are examples of how UAVs can contribute to social well-being and security in several fields of life. New services and solutions will be available in the future. The development of the technology can't be stopped, but future applications will face new challenges and restrictions that are out of sight today.

Social and well-being aspects should be taken into consideration because the decreasing service fees and increasing accessibility of the service will result in massive needs. It will mean that many devices (UAVs) will fly over the cities in the low-level airspaces. Will society tolerate the noise pollution of

the ever-moving, freight-carrying UAV traffic in the suburbs? Now, this seems like a utopian idea, but there may soon come a time when people can hear only the noise of UAS instead of the bees' buzzes and birds' songs when they are sitting in the garden.

AUTHOR CONTRIBUTIONS

Z. Sándor: Conceptualization, Experiments, Theoretical analysis, Writing, Review and editing.

DISCLOSURE STATEMENT

The authors declare that they have no known competing financial interests or personal relationships that could have appeared to influence the work reported in this paper.

ORCID

Zsolt Sándor <http://orcid.org/0000-0002-6969-5192>

REFERENCES

- [1] Anshul Yadav, Salil Goel, Bharat Lohani & Shubhanshi Singh (2021) „A UAV Traffic Management System for India: Requirement and Preliminary Analysis”, *J Indian Soc Remote Sens* 49, pp. 515–525. <https://doi.org/10.1007/s12524-020-01226-0>
- [2] Schroth, L. “The Drone Market 2019–2024: 5 Things You Need to Know”, [online] Available at: <https://droneii.com/the-drone-market-2019-2024-5-things-you-need-to-know> [Accessed: 15 May 2021].
- [3] Gupta, Anunay, Tanzina Afrin, Evan Scully, and Nita Yodo (2021) "Advances of UAVs toward Future Transportation: The State-of-the-Art, Challenges, and Opportunities" *Future Transportation* 1, no. 2: 326-350. <https://doi.org/10.3390/futuretransp1020019>
- [4] Sylverken AA, Owusu M, Agbavor B, Kwarteng A, Ayisi-Boateng NK, Ofori P, et al. (2022) “Using drones to transport suspected COVID-19 samples; experiences from the second largest testing centre in Ghana, West Africa”. *PLoS ONE* 17(11): e0277057. <https://doi.org/10.1371/journal.pone.0277057>
- [5] E. Ackerman and E. Strickland (2018), "Medical delivery drones take flight in east africa," in *IEEE Spectrum*, vol. 55, no. 1, pp. 34-35, <https://doi.org/10.1109/MSPEC.2018.8241731>
- [6] Emmanuel Lamptey, Dorcas Serwaa (2020) “The Use of Zipline Drones Technology for COVID-19 Samples Transportation in Ghana” *HighTech and Innovation Journal* Vol. 1, No. 2, June, 2020 <https://doi.org/10.28991/HIJ-2020-01-02-03>
- [7] Valuates Reports “Drone Logistics and Transportation Market Size to Reach USD 10,990 Million by 2026 at CAGR 10.8%”, [online] Available at: <https://www.prnewswire.com/in/news-releases/drone-logistics-and-transportation-market-size-to-reach-usd-10-990-million-by-2026-at-cagr-10-8-valuates-reports-857193310.html> [Accessed: 5 Nov 2022]
- [8] GLOBE NEWSWIRE “Drone Package Delivery Market to Hit USD 7,388.2 Million by 2027”, [online] Available at: <https://www.globenewswire.com/news-release/2020/11/30/2136699/0/en/Drone-Package-Delivery-Market-to-Hit-USD-7-388-2-Million-by-2027-Diverse-Entities-Such-as-Amazon-and-FedEx-to-Explore-Wider-Delivery-Applications-of-Drones-States-Fortune-Business-.html> [Accessed: 5 Nov 2022]
- [9] Fortunebusinessinsights “Drone Package Delivery Market Size” [online] Available at: <https://www.fortunebusinessinsights.com/drone-package-delivery-market-104332> [Accessed: 5 Nov 2022]
- [10] Mohamed Nadir Boukoberine, Zhibin Zhou, Mohamed Benbouzid (2019) “Power Supply Architectures for Drones - A Review”. In *IECON 2019 - 45th Annual Conference of the IEEE Industrial Electronics Society*. IEEE

- Press, 5826–5831.
<https://doi.org/10.1109/IECON.2019.8927702>
- [11] Boukoherine, N.M.; Zhou, Z.; Benbouzid, M. Power supply architectures for drones—A review. In Proceedings of the IECON 2019-45th Annual Conference of the IEEE Industrial Electronics Society, Lis-bon, Portugal, 14–17 October 2019.
<https://doi.org/10.1109/IECON.2019.8927702>
- [12] Kris Yowtak, Justin Imiola, Michael Andrews, Keith Cardillo, Steven Skerlos (2020) "Comparative life cycle assessment of unmanned aerial vehicles, internal combustion engine vehicles and battery electric vehicles for grocery delivery" *Procedia CIRP*, Volume 90, pp 244-250, ISSN 2212-8271,
<https://doi.org/10.1016/j.procir.2020.02.003>
- [13] Aurambout, JP., Gkoumas, K. & Ciuffo, B. (2019) "Last mile delivery by drones: an estimation of viable market potential and access to citizens across European cities" *Eur. Transp. Res. Rev.* 11, 30.
<https://doi.org/10.1186/s12544-019-0368-2>
- [14] Businessinsider "Amazon's Prime Air Drone Deliveries to Cost \$63 Per Package" [online] Available at:
<https://www.businessinsider.com/amazon-prime-air-drone-delivery-cost-63-per-package-2025-2022-4> [Accessed: 5 Nov 2022]
- [15] Constantine Samaras, Joshua Stolaroff "Is Drone Delivery Good for the Environment?" [online] Available at:
<https://www.smithsonianmag.com/innovation/drone-delivery-good-for-environment-180968157/> [Accessed: 5 Nov 2022]
- [16] Packaging Europe "How drones are reshaping home delivery" [online] Available at:
<https://packagingeurope.com/how-drones-are-reshaping-home-delivery/4009.article> [Accessed: 5 Nov 2022]
- [17] Stefano Magistretti, Claudio Dell'Era (2019) "Unveiling opportunities afforded by emerging technologies: evidences from the drone industry", *Technology Analysis & Strategic Management*, 31:5, 606-623,
<https://doi.org/10.1080/09537325.2018.1538497>
- [18] Commission Implementing Regulation (EU) 2019/947 of 24 May 2019 on the rules and procedures for the operation of unmanned aircraft, Bruxelles, Netherlands, [online] Available at: https://eur-lex.europa.eu/eli/reg_impl/2019/947/oj [Accessed: 5 Nov 2022]
- [19] European Union Aviation Safety Agency (2022) "Acceptable Means of Compliance (AMC) and Guidance Material (GM) to Commission Implementing Regulation (EU) 2019/947" Bruxelles, Netherlands, [online] Available at:
<https://www.easa.europa.eu/en/downloads/110913/en> [Accessed: 5 Nov 2022]
- [20] Roca-Riu, Mireia, Menendez, Monica "Logistic deliveries with drones - State of the art of practice and research", 19th Swiss Transport Research Conference (STRC 2019), Ascona, Switzerland, May 15-17, 2019.
<https://doi.org/10.3929/ethz-b-000342823>
- [21] Demuyakor, J (2020) "Ghana Go Digital Agenda: The impact of Zipline Drone Technology on Digital Emergency Health Delivery in Ghana." *Shanlax International Journal of Arts, Science and Humanities*, vol. 8, no. 1, pp. 242–253. DOI:
<https://doi.org/10.34293/sijash.v8i1.3301>
- [22] Gangwal, A, Akshika Jain and S. Mohanta. (2019) "Blood Delivery by Drones: A Case Study on Zipline.". *International Journal of Innovative Research in Science, Engineering and Technology* Vol. 8, Issue 8, August 2019.
http://www.ijirset.com/upload/2019/august/63_Blood.PDF
- [23] Tele 2 IoT: Everdrone: Delivering Critical Medical Care By Drone [online] Available at:
<https://tele2iot.com/case/everdrone-delivering-critical-medical-care-by-drone/> [Accessed: 5 Nov 2022]
- [24] EverDrone: For the first time in medical history, an autonomous drone helps save the life of a cardiac arrest patient PRESS RELEASE 04.01.2022 Drone [online] Available at:
<https://everdrone.com/news/2022/01/04/for-the-first-time-in-medical-history-an-autonomous-drone-helps-save-the-life-of-a-cardiac-arrest-patient/> [Accessed: 5 Nov 2022]
- [25] Lykou, Georgia, Dimitrios Moustakas, and Dimitris Gritzalis. (2020). "Defending Airports from UAS: A Survey on Cyber-Attacks and Counter-Drone Sensing Technologies" *Sensors* 20, no. 12: 3537.
<https://doi.org/10.3390/s20123537>
- [26] Willassen, Harald Remi & Loedding, Erik & Knutsen, Axel, 2020. "Drones at Oslo Airport, Norway: A case study on how to balance safety and business development," *Journal of Airport Management*, Henry Stewart Publications, vol. 14(3), pages 260-268, June. Handle:
<https://ideas.repec.org/a/aza/jam000/y2020v14i3p260-268.html>
- [27] Pyrgies, J. (2019). "The UAVs threat to airport security: Risk analysis and mitigation" *Journal of Airline and Airport Management*, 9(2), 63-96. <https://doi.org/10.3926/jairm.127>
- [28] Konert, A., Kasprzyk, P. (2021) "UAS Safety Operation – Legal Issues on Reporting UAS Incidents" *J Intell Robot Syst* 103, 51
<https://doi.org/10.1007/s10846-021-01448-5>
- [29] Shvetsova, S.V., Shvetsov, A.V. (2021) Ensuring safety and security in employing

- drones at airports. *J Transp Secur* 14, 41–53
<https://doi.org/10.1007/s12198-020-00225-z>
- [30] Callaway Climate Insights, Sally French “Is Amazon drone delivery really all that environmentally friendly?” [online] Available at:
<https://www.callawayclimateinsights.com/p/is-amazon-drone-delivery-really-all> [Accessed: 5 Nov 2022]
- [31] City Logistics “Delivery drones: sustainable or not?” [online] Available at:
<http://www.citylogistics.info/research/delivery-drones-sustainable-or-not/> [Accessed: 5 Nov 2022]
- [32] Wonsang Yoo, Eun Yu, Jaemin Jung (2018) “Drone delivery: Factors affecting the public’s attitude and in-tention to adopt” *Telematics and Informatics*. Volume 35, Issue 6, pp 1687-1700, ISSN 0736-5853,
<https://doi.org/10.1016/j.tele.2018.04.014>



This article is an open access article distributed under the terms and conditions of the Creative Commons Attribution NonCommercial (CC BY-NC 4.0) license.

Analysis of coupling system failures on freight trains

Marija Vukšić Popović^{1,*}, Jovan Tanasković², Zorica Starčević³, Nebojša Mededović³

¹Department School of Railroad Transport, Academy of Technical and Art Applied Studies Belgrade
Zdravka Čelara Str., 14, Belgrade, 11000, Serbia

² Department of Rail Vehicles, Faculty of Mechanical Engineering, University of Belgrade
Kraljice Marije Str., 16, Belgrade, 11000, Serbia

³Joint Stock Company for Freight Railway Transport "Serbia Cargo" Belgrade
Nemanjina Str., 6, Belgrade, 11000, Serbia

*e-mail: marija.vuksic.popovic@vzs.edu.rs

Submitted: 26/01/2023 Accepted: 16/02/2023 Published online: 22/02/2023

Abstract: This paper presents an analysis of train coupling failure that led to trains break apart on the Serbian Railways over 10 years period. Train coupling failure of freight trains with single locomotives was considered. The analysis was done based on accident data combine with FMECA risk assessment. As a result distribution of failure along the train, driving regime and velocity were obtained, as well as the frequency of failure concerning the length and mass of the trains, load status, etc. The systematization of coupling failure helped to establish conditions leading to failure and to define the parameters causing it. Risk factors for coupling failure were determined using FMECA risk assessment. Preventive measures are recommended for the revision of maintenance. Risk analysis of coupling system failure can be different depending on the time of analysis (regulations, exploitation conditions) and the applied maintenance practice. FMECA analysis applied to train coupling systems based on regulation shows different permissible risk values that don't match exploitation data.

Keywords: coupling system failure; railway; risk analysis; train breaks apart

I. INTRODUCTION

The coupling system of freight trains on Serbian railways, like in other European countries, consists of a screw coupler and draw gear (**Fig. 1**), while a majority of railways outside Europe use automatic couplers. They provide mechanical connections that transmit traction forces between vehicles along the train. Train coupling failure analysis aimed to classify coupling failure cases with causes, circumstances and consequences. Analysis can determine what leads to failure increase. Since coupling failure can have a safety impact on railway traffic by causing trains to break apart, it is primary to predict coupling failure and propose measures to reduce them.

According to EU Directive 2016/798 [1], train breaks apart are classified as incidents and are not recorded in the Rail accidents database [2] to the ERA (European Union Agency for Railways). Analyzes of individual cases of train breaks apart were carried out, with an emphasis on determining the cause of coupling system failure and the root cause analysis [3-8].

From 2016 to 2020 railway operator in freight traffic "Serbia Cargo" had an average of 36,4 cases per year of coupling failures [9, 10]. Total number of accidents on the Serbian railway from 2016 decrease relative to previous years, as well as the number of coupling failures that was 40,2 cases [9, 11] per year (from 2007 to 2011). Although the total number of accidents decrease, the number of train coupling failures relatively increased by almost 14% [12].

The rolling stock of railway operator "Serbia Cargo" in 2020 was reduced by almost 43% relative to the stock of national operator "Serbian Railways" ("Serbia Cargo" legal predecessor) from 2007. The number of freight wagons was, also, reduced by approx. 53% [12]. The rolling stock (on average) is over 40 years old, and a large number of vehicles are rented from other railway operators in Europe. Also, there are a certain number of foreign vehicles, running according to the GCU (General Contract of Use for Wagons). Considering the previous, analysis of train coupling failure on Serbian railways does not have a purely national character and is not defined.

The risk of trains breaking apart, caused by coupling failure, in railway traffic is a quantitative

measure of the severity, detectability and frequency. Taking measures to reduce coupling failure is to manage improvement through preventive maintenance, quality, design and operation [13].

Risk analysis of coupling failure was made based on the EN 50126 series standards [14, 15] for railway applications of RAMS management (Reliability, Availability, Maintainability and Safety). Failures are ranked according to the criticality level, known as the Risk Priority Number (RPN). Failure Mode and Effects and Criticality Analysis (FMECA) is based on Failure Mode and Effects Analysis (FMEA) with the additional critical analysis performed after the implemented FMEA.

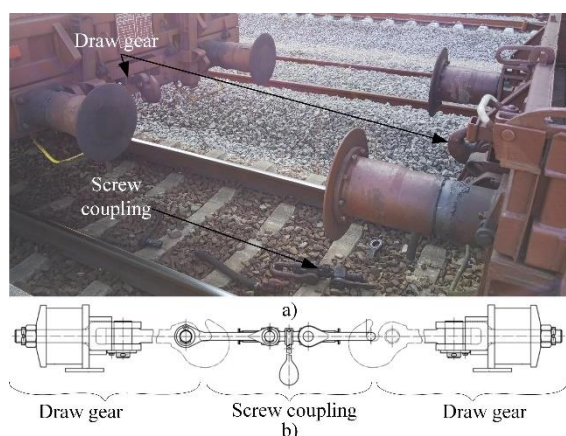


Figure 1. Coupling system on freight trains, a) at train brakes apart, b) schematic view between 2 wagons

II. METHODS

1. FMECA method

The ranking of the severity, detectability and frequency of coupling failure for freight wagons was made according to ranks in UIC B169, RP 43 [13], where the rank have values from 1 to 10. For severity, values range from „no impact“ for 1 rank to „unsafe without warning“ for rank 10. The ranking of detectability of failures goes from „nearly certain“ for rank 1 to „nearly uncertain“ for value 10. The frequency range has values from rank 1 „little - failure is implausible“ for a value less than 10^{-9} to „very high: Failures in very short cycle which are not avoidable“ for a value more than $8 \cdot 10^{-3}$ per year for rank 10 [13].

Risk evaluation is the assessment of the obtained RPN with the limited RPN value, defined in the risk analysis process, to identify the criticality level with increased risk. If the calculated RPN is above the set limit value, it is considered unacceptable and improvement measures must be implemented. If the RPN is below the set limit value, but it is not negligible, it is considered conditionally acceptable and only economically justified measures are applied

[16]. The rank of severity (S), detectability (D) and frequency (F) have values between 1 and 10, so the risk evolution in RPN range from 1 to 1000.

Some failure of mechanical components could, due to deterioration over time, become causes of severe failure. Failure means that the observed object can no longer perform the function and realize the operating conditions. The quality deteriorating of the component does not mean failure, but some failures can become failure root causes [13]. For the coupling system of freight wagons in railway operator "Serbia Cargo", consisting of screw coupling and draw gear, quantitative values of failure can be obtained, based on accidents reports.

For one or more components of the coupling system, due to the deterioration of their condition over time (wear, corrosion, etc.) or overload, severity could progressively increase. Using experience and data from an operation, taking into account the worst outcome in the failure chain for all components, the result is always coupling failure leading to trains breaking apart. Thus, the risk analysis was significantly cut by the assessment of component failures (fractures) only. Results of risk analysis of the coupling system of "Serbia Cargo" freight wagons were based on the number, equipment and technical condition of the vehicles in use from 2018 to 2020. The introduction of an Entity in Charge of Maintenance (ECM) in railway maintenance and reconstruction of the Serbian railway company in 2015 into 3 separate entities with changing and aging of rolling stock, affected characteristics of train coupling failure.

2. Method for prediction of train breaks

The relative indicator of train breaks apart in railway freight traffic is the ratio of the number of train breaks and the traffic volume in millions of tonne-kilometre. This relative indicator represents the frequency of train breaks apart reduced to ton-km per year. Based on the determined frequency of train breaks apart and their effects on railway traffic in recent years, it was possible to predict the risk of train breaks accordingly. The prediction was based on data obtained for equal or similar [16]:

- types of vehicles (wagons and engines) and their condition (quality and maintenance),
- traffic condition,
- train driving and
- external and other conditions in operation.

3. Method for train breaks data analysis

In train breaks apart analysis various methods were applied for the classification of failure cases and systematization of operational data [10]. The induction method, aiming to review the circumstances that preceded the coupling failure, was based on the investigation reports along with

exploitation and maintenance experience. Based on the conducted analysis coupling failure factors were defined. The collected data and information were processed statistically to quantify the factors. Using the generalization method, the most important causes of coupling failures and the critical parts of the coupling system were determined. The analysis of coupling failure cases shows the frequency of failure so that preventive measures can be proposed to focus on reducing train breaks apart. During the analysis of train breaks apart cases, it was not possible always to determine all primary characteristics due to data deficiencies or insufficiency.

The analysis of relevant cases of train breaks apart was carried out from 2 main aspects:

- causes and
- effects.

Other aspects of train breaks apart include:

- the distribution of coupling failure along the train,
- driving mode before train breaks apart,
- train speeds before train breaks apart,
- characteristics of trains that break apart (number of wagons, length and weight of the train), etc.

III. RESULTS AND ANALYSIS

4. FMECA risk assessment

The analysis of the risk of coupling failure showed that the RPN is the highest for component failure with the direct consequence of the train breaking apart. As the severity for all component failures is equal, the RPN depends on detectability and frequency. RPN value was limited at 250 according to the EN 50126 series standard [14, 15]. The most critical component failures were [16]: drawbar (RPN = 400), draw hook (RPN = 320), coupling links, screw and joint pin (RPN = 288), elastic device (RPN = 280), coupling head and hose and brake pipe (RPN = 256). Prime critical components have high frequency and low detectability in operation due to the inaccessibility of components in the preventive inspection.

5. Prediction of train breaks

Limitations of train breaks apart predictions are assigned data for particular railway vehicles and traffic conditions. For parameters change, the projection will not correspond to the attained data. The model of a prediction was made for train breaks apart of the operator "Serbia Cargo" in 2020, based on the breaks frequency from 2016 to 2019.

The average frequency of train breaks apart reduced to ton-km per year between 2016-2019 amounts to 0,0079 breaks/mil. ton-km per year [9, 15]. For the realized volume of 4,178 million ton-km freight traffic of "Serbia Cargo" in 2020, it can be

predicted 33 cases of train breaks apart (**Fig. 2**). Only 24 cases in 2020 were registered. The reduction of train breaks number as much as 37% compared to the previous years is not unexpected, when it's known that decreasing trend is almost 28% for all accidents and incidents from 2010 [16]. The decrease in the number of trains breaking apart and the total number of accidents and incidents were only a partial effect of the decrease of 8% in traffic volume in 2020, compared to 2019.

Based on the presented data, it is the evident influence of the newly-formed Accident and incident analysis team within the safety management system of "Serbia Cargo" at the end of 2019. The team's focus was to re-analyze all accidents and incidents after submitting the final investigation reports. The team proposes improvement measures for increasing traffic safety. The establishment of an Accident and incident analysis team resulted in greater responsibility for all participants involved in the railway traffic. A decrease in the total number of accidents and incidents, and therefore train breaks apart, have an effect due to the implementation of measures and security recommendations of the team and the entire security management system.

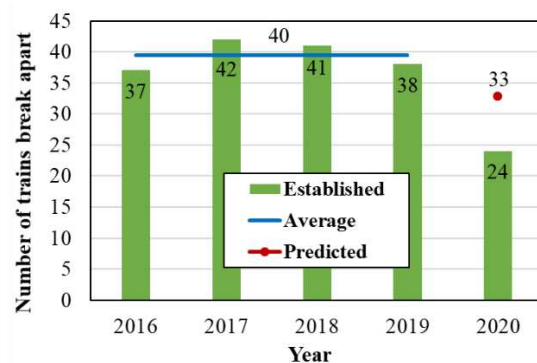


Figure 2. Prediction of train break apart frequency

6. Train breaks data analysis

The trains break apart is a result of coupling system failure. The official analysis of coupling system failure on Serbian railway, states that the cause of failure, in over 50% of cases, was the fatigue of material (**Fig. 3**), such as changed material structure, loss of connection parts, and other irregularities related to the material. Irregularities in driving are listed in 15% to 18% of cases as the cause of trains break apart [12]. Variations of train composition, tightness of screw coupling, as well as the vehicle condition make 9% to 20% of trains break apart causes. The increase of the material in the last ten years, as the main cause of coupling failures from 51% to 60% cases, considered independently, indicates that there has been a decrease in the quality of diagnostics in the maintenance of coupling systems.

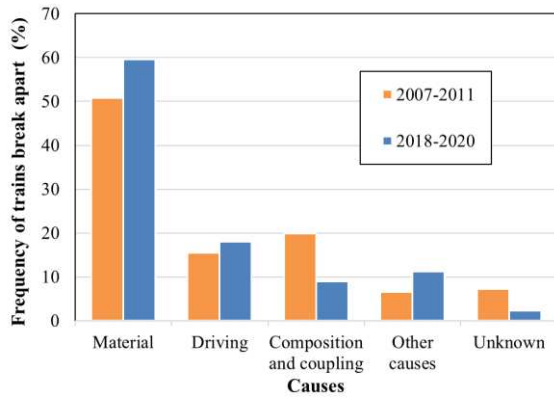


Figure 3. Causes of trains break apart

In 55% cases the reason for coupling failures were parts of the draw gear and coupler in 37% of cases (Fig. 4). The failure of other parts was significantly less - about 8%. From 2018 the failure of draw gear elements has increased to 64%, while the failure of coupler elements has decreased to 27% [12].

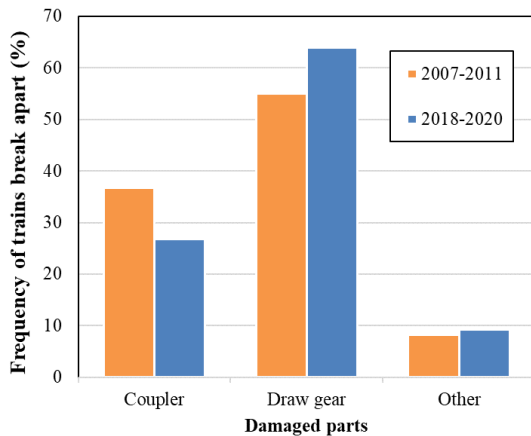


Figure 4. Damaged parts when trains break apart

The consequences of the coupling failure and train breaking apart are direct costs of the material (spare parts and repair), but can also include indirect costs (delay of a broken train and other trains on the line). Additional costs are related to traffic disruption and organizational change. From 2007 to 2011, the direct material costs of breaking trains apart were up to 1000 euro, and the traffic closure on the rail line section lasted on average 3 to 4 hours [9]. Similar was from 2018 to 2020, with direct material costs between 400 and 900 euros, and the traffic closure between 4 and 5 hours (Fig. 5) [9]. These consequences do not include the total costs of keeping trains and the engaged train route, which do not happen at every break, but can amount to 3000 euro and higher.

The conditions of technical inspection and the level of the technical quality of wagons in the exchange between railways in Europe are defined in Annex 9 of GCU. Annex 9 refers to all the damages caused by the accident, and new fractures (without fatigue signs), to inadequate handling of train by the

railway operators. Therefore coupling failure can have significant financial consequences as all fractures during train breaks, in which there are no clear traces of fatigue, or wear on broken parts, are considered the responsibility of the railway operator.

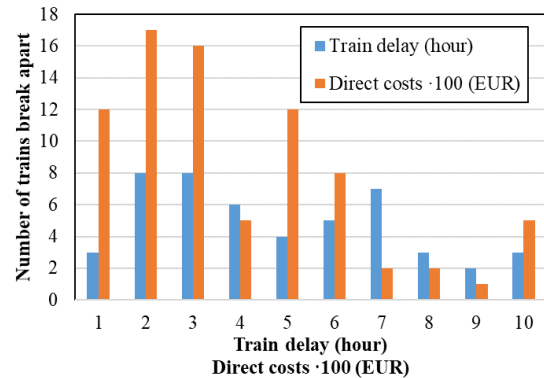


Figure 5. Train delay after the break

A decade ago, as many as 59% of cases of coupling failure on freight trains were on the first third of the train length (Fig. 6) of which 26% are coupling failures between the locomotive and the first wagon, and 33% between the first wagon and the first third of the train length. Only 18% of train coupling failures were between the first and second third of the train length. A rather different distribution of coupling failure was in recent years, where in 38% of cases coupling failures were on the first third of the train length (Fig. 6), of which 16% are coupling failures between the locomotive and the first wagon. Almost 40% of coupling failures were on the second third of the train length compared to just 11% on the last third [9].

A large number of coupling failures between the locomotive and the first wagon leads to locomotive damage. Over 50% of damaged locomotives can't be repaired in operation, thereby increasing the expenses of the incident and can lead to traffic closure.

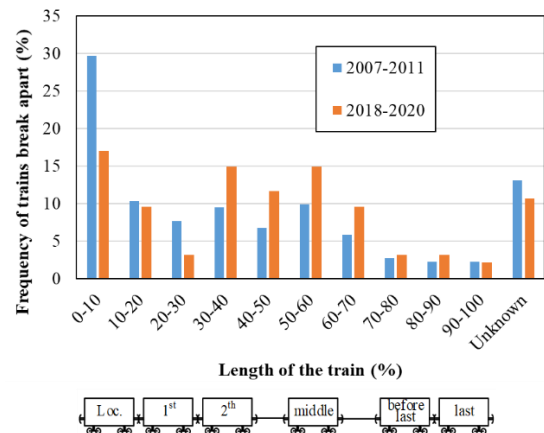


Figure 6. The distribution of trains break apart along the train

Coupling failure between the locomotive and the first wagon mostly occurs during traction, while other cases mainly occur during braking or changing of direction. From 2018 to 2020 decrease in the number of coupling failures in the front part of the train, and increasing in the middle of the train (Fig. 6), was caused by a larger number of coupling failures during maneuvers (pushing) that were taken into account.

Braking, from all driving modes, has the most significant effect on coupling failures, mostly due to large longitudinal forces, and from 2007 to 2011 caused 56% of cases of failures. In recent years, from 2018 to 2020, the effect of braking as the cause of coupling failures decrease to 41% (Fig. 7). Pulling has same effect on coupling failure (20% to 23%), while maneuvering caused more coupling failure recently [12].

Ten years ago coupling failure mostly occurred at train speed between 10 and 20 km/h (34% cases - Fig. 8) [9], while recently most coupling failures occurred at speeds up to 10 km/h (39%). The number of coupling failures decreases with increasing speed, so as many as 58 ÷ 65% of coupling failures occur at speeds less than 20 km/h (Fig. 8) [12].

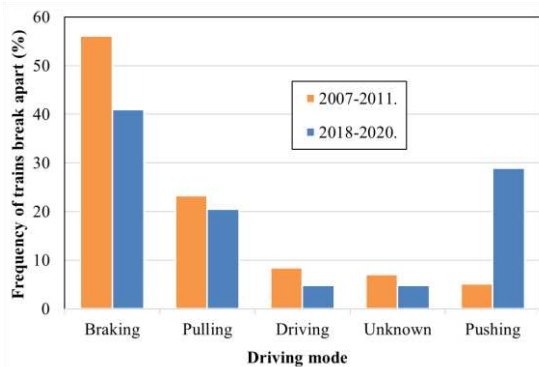


Figure 7. Driving mode before trains break apart

Almost 50% to 70% of train coupling failures occur in the station area or switchyards because of a more frequent number of starts and stops (therefore traction and braking), which implies low speeds in stations and nearby.

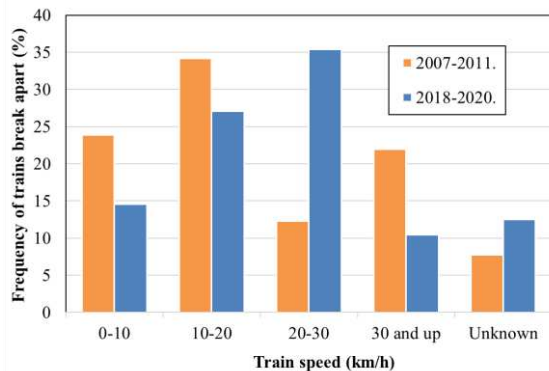


Figure 8. Train speed before trains break apart

The frequency of coupling failure can be influenced by train parameters, like the number of wagons, the length and weight of the train, the state of loading, the schedule of loaded and empty wagons in the train, and others. The coupling failure occurs in freight trains with a small number of wagons (8 to 15) and a large number of wagons (43 to 51). In the last few years coupling failures occurred most frequently in trains with 20 to 35 wagons (Fig. 9).

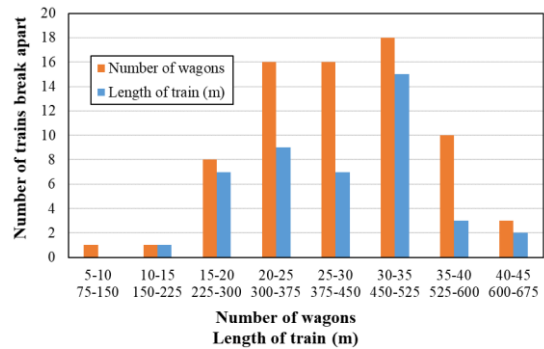


Figure 9. Number of wagons and length of trains of trains break apart

Consequently, as average freight train in the last ten years had 26 to 27 wagons [9], length of broken trains ranged from 152 m to 720 m. The average length of trains breaking apart was about 400 m. It can be concluded that the frequency of train coupling failure increases with train length over 500 m (Fig. 9).

The masses of trains that have coupling failure range from 336 t to 2333 t (Fig. 10). The average gross weight of one train in 2009 was 926 t [9], and of a train that break apart 1354 t, similar to the last few years.

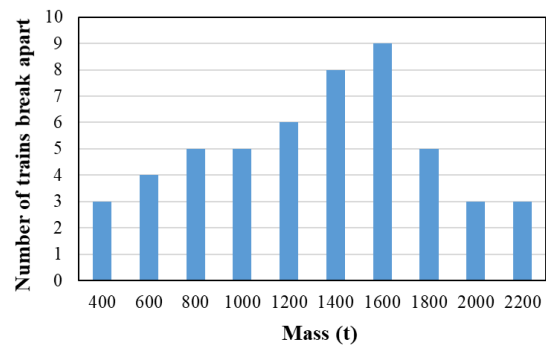


Figure 10. Mass of trains break apart

The frequency of coupling failure is somewhat higher for trains with all loaded wagons (27%) related to 16% for trains with all empty wagons. Trains with diverse lodes (both loaded and empty wagons) have 25% frequency of coupling failure, but in almost a third of cases loading data were not available.

IV. CONCLUSIONS

The cause of the train breaking apart is coupling failure. Separated parts of the train are automatically stopped, but failure could lead to an increase in stopping distance and passing through a signal or crossing. Although it seems that consequences of coupling failure have relatively low severity in everyday practice, as a safety precaution, all measures must be applied to reduce causes of train break apart. Taking measures to reduce or eliminate the causes of coupling failure is to manage the risk of the train breaking apart usually by preventive maintenance, quality, design and operation.

The characteristics of train coupling failure observed over a decade show a decrease of locomotive damage and frequency of coupling failure in the front part of a train, as well as an increase of coupler and draw gear fatigue. Since coupling and draw gear are standard constructions, and also inspected with regular maintenance, the percentage of failure caused by material fatigue is extensive. Significantly, the frequency of coupling failure due to train driving has not decreased.

To increase the safety of railway traffic, monitoring and analysis of common safety indicators must be performed. Risk assessment should be performed by the railway infrastructure management or railway undertakers and through the review of changes in the railway network and analysis of

railway safety in the previous period and the need to implement measures to reduce risk.

ACKNOWLEDGEMENT

The publishing of this paper was supported by management of the railway operator "Serbia Cargo" and Ministry of Education, Science and Technological Development of Republic of Serbia, Project Contract 451-03-9/2022-14/200105.

AUTHOR CONTRIBUTIONS

M. Vukšić Popović: Conceptualization, Data analysis, Finite element modelling, Writing.

J. Tanasković: Review and editing, Supervision.

Z. Starčević: Data collection and analysis, Review and editing.

N. Mededović: Data collection and analysis, Review and editing.

DISCLOSURE STATEMENT

The authors declare that they have no known competing financial interests or personal relationships that could have appeared to influence the work reported in this paper.

REFERENCES

- [1] Directive (EU) 2016/798 of the European Parliament and of the Council of 11 May 2016 on railway safety, Official Journal of the European Union, L 138/102. <https://eur-lex.europa.eu/legal-content/EN/TXT/?uri=CELEX:02016L0798-20201023>
- [2] Rail accidents by type of accident (ERA data), Eurostat, https://ec.europa.eu/eurostat/databrowser/view/TRAN_SF_RAILAC_custom_4989745/default/table?lang=en
- [3] V. Infante, C. M. Branco, et al., A failure analysis study of cast steel railway couplings used for coal transportation. Engineering Failure Analysis 10 (4) (2003). [https://doi.org/10.1016/S1350-6307\(03\)00012-8](https://doi.org/10.1016/S1350-6307(03)00012-8)
- [4] M. Mohammadi, A. Rahmatfam, et al., Failure analysis study of railway draw-hook coupler, Journal of Central South University, (26) (2019) pp. 916–924. <http://dx.doi.org/10.1007/s11771-019-4060-4>
- [5] A. Cernescu, I. Dumitru, et al., The analysis of a damaged component from the connection system of the wagons, Engineering Failure Analysis, (29) (2013) pp. 93–107. <https://doi.org/10.1016/j.engfailanal.2012.11.009>
- [6] F. Nový, M. Jambor, et al., Investigation of the brittle fracture of the locomotive draw hook, Engineering Failure Analysis, (105) (2019) pp. 305–312. <https://doi.org/10.1016/j.engfailanal.2019.07.019>
- [7] R. Ulewicz, F. Nový, et al., The investigation of the fatigue failure of passenger carriage drawhook, Engineering Failure Analysis, Elsevier Ltd. (104) (2019) pp. 609–616. <https://doi.org/10.1016/j.engfailanal.2019.06.036>
- [8] M. Vukšić Popović, J. Tanasković, et al., Experimental and numerical research on the failure of railway vehicles coupling links, Engineering Failure Analysis, (127) (2021), 105497, ISSN 1350-6307. <https://doi.org/10.1016/j.engfailanal.2021.105497>

M. Vukšić Popović, Failure analysis of draw gear and screw coupling of railway vehicles as a factor of safety and trains break risk, Ph.D. thesis, University of Belgrade Faculty of Mechanical Engineering, (2021), in Serbian.

- <https://nardus.mpn.gov.rs/handle/123456789/18628>
- [9] Statistical report on accidents and incidents in „Serbia Cargo“, <https://www.srbcargo.rs/sr/statisticki-izvestaji-o-nesrecama-i-nezgodama/>
- [10] Traffic and safety reports of rail transport on Serbian Railways, „Serbian Railways“, Belgrade, 2013.
- [11] M. Vukšić Popović, J. Tanasković, et al., The trend of train coupling failure on Serbian railways in 10 year period, XX International Scientific-Expert Conference on Railway RAILCON '22, Niš, Serbia, 2022, pp. 109-112. <https://railcon.rs/Proceedings/Railcon 22 Conference Proceedings.pdf>
- [12] Guideline: Reliability, availability, maintainability, safety - Implementation of EN 50126 for Mechanical Components in Railway, UIC B 169/RP 43 RAMS (2015).
- [13] Railway Applications - The Specification and Demonstration of Reliability, Availability, Maintainability and Safety (RAMS) - Part 1: Generic RAMS Process, EN 50126-1:2017 (2017).
- [14] Railway applications - Specification and demonstration of Reliability, Availability, Maintainability and Safety (RAMS) Part 2: Systems Approach to Safety, EN 50126-2:2019 (2019).
- [15] M. Vukšić Popović, J. Tanasković, Z. Starčević, Risk assessment of coupling system failure on train in current maintenance system, XX International Scientific-Expert Conference on Railway RAILCON '22, Niš, Serbia, 2022, pp. 117-120. <https://railcon.rs/Proceedings/Railcon 22 Conference Proceedings.pdf>



This article is an open access article distributed under the terms and conditions of the Creative Commons Attribution NonCommercial (CC BY-NC 4.0) license.

Performance assessment of full depth asphalt pavements manufactured with high recycled asphalt pavement content

Csaba Toth^{1,*}, Laszlo Petho², Szabolcs Rosta³, Peter Primusz¹

¹Department of Highway and Railway Engineering, Budapest University of Technology and Economics
Műegyetem rakpart 3, 1111 Budapest, Hungary

²Fulton Hogan Infrastructure Services
180 Burnside Road, Ormeau, 4208, QLD, Australia

³Duna Group
Nagy Jenő u. 12., 1126 Budapest, Hungary

*e-mail: toth.csaba@epito.bme.hu

Submitted: 05/02/2023 Accepted: 15/02/2023 Published online: 22/02/2023

Abstract: Reclaimed asphalt pavement (RAP) is generated during road rehabilitation and resurfacing projects. This highly valuable recycled material should be used for manufacturing fresh hot mix asphalt (HMA) for new asphalt pavement layers to ensure the highest added value and minimise environmental impact. The use of RAP is already common practice worldwide; however, incorporating RAP into the manufacturing of HMA is still very minimal in Hungary. As part of a research work HMA containing 20-50% RAP was designed, manufactured and tested. This paper discusses the performance tests carried out on laboratory and plant mixed asphalt mixes; using this data the overall full depth asphalt (FDA) pavement performance was predicted through general mechanistic pavement design. The outcomes of this paper showed that high RAP content asphalt mixes can have superior performance; this disproves the common perception that high RAP mixes are substandard road construction materials. The analysis performed in this paper found that asphalt mixes with high RAP content present low risk for in-situ performance. However, in order to achieve this outcome, the application of correct mix design methodology, appropriate RAP management and suitable asphalt plant capability for mass production are paramount.

Keywords: *performance; pavement design; recycled asphalt pavement*

I. INTRODUCTION

Reclaimed asphalt pavement (RAP) is generated during road rehabilitation and resurfacing projects through cold milling or breaking up layers, which is quite often used then for lower base layer or shoulder works in Hungary. This approach is not considered the best application from a national economy perspective, as it should be ensured that recycled materials are incorporated into newly constructed road pavement layers at the highest possible level, i.e. road base material in road base and asphalt material in asphalt layers. This is to ensure that the energy embedded in the relevant layer during the original manufacturing and construction activity is not lost or the loss is minimised. The most obvious solution to this problem is the use of asphalt mixes manufactured with the addition of RAP.

The use of RAP is already common worldwide at a fairly large level in the asphalt lower base, base and

intermediate (binder) layers; there is still a lot of potential increasing the RAP content especially in the wearing course applications [1].

Unfortunately incorporating RAP into the manufacturing of new hot mix asphalt (HMA) is still very minimal in Hungary, despite the obvious economic advantages and developments in asphalt manufacturing technologies in the last two decades. In Germany and France huge quantities of RAP have been used for the production of HMA at asphalt mixing plants. Based on latest figures from the European Asphalt Pavement Association [2], 11.6 million tons of RAP was used in Germany and 6 million tons in France in 2021. In Hungary, this volume was 157,000 tons, which means that in average only 3.2% of the total asphalt production contained RAP. The average recycling rate in Germany was 25.6%, while in France this value was 12.8%. **Table 1** provides a summary of these figures where the neighbour country, Austria is also

highlighted; average RAP usage was 10.5% in Austria. In the United States (US) RAP usage increased from an average of 15.6% in 2009 to an average of 21.9% in 2021. Given the US is a very large country with an extensive road network the total RAP usage was accordingly a total of 94.6 million tonnes in 2021 [3]. A study tour conducted by US researchers in December 2014 in Japan revealed that the country produces 55 million tonnes of asphalt and the average RAP usage was 47%. There was a significant increment in usage since 2000 when the average RAP usage was 33% [4]. No recent has been data published for Japan, therefore this latest data set was not added to the summary (Table 1).

Table 1. Hot mix asphalt and recycled asphalt pavement usage in various countries in 2021

Country	Total RAP used in asphalt (Mt)	Total asphalt (Mt)	Average RAP in asphalt mixes (%)
Hungary	0.16	4.9	3.2
Germany	9.7	38.0	25.6
France	4.6	35.9	12.8
Austria	0.8	7.3	10.5
US	94.6	432.0	21.9

While many asphalt plants are capable to incorporate 10-15% RAP in Hungary, these limits are not being utilized otherwise 490,000 to 735,000 tonnes of RAP would have been used in 2021. In 2022 an asphalt plant was established in Hungary capable for the addition of RAP up to 60% by using some of the latest technological advancements in hot mix asphalt production. When adding RAP to HMA, some of the economic and environmental benefits are the reduction of primary raw materials, such as crushed stone, bitumen and additives; this also minimizes transport costs. These altogether result in the reduction of the overall carbon footprint of asphalt manufacturing and laying and other greenhouse gases emitted during production.

Within the framework of a research and development project, an asphalt mixing plant was established for the production of asphalt mixtures with a high RAP content. During the project the complex system of large-scale production was established, innovative laboratory testing and mix design was developed and a monitoring system was implemented. Asphalt recycling has several measurable advantages as follow:

- Minimizing the consumption of new bitumen
- Reducing the rate of use of new crushed stone and ground limestone or filler
- Lower energy costs
- Decreasing environmental loading

- Identical asphalt quality if designed and controlled correctly.

Within the framework of the project, RAP stockpile management was considered, such as preparation, processing and storage of processed RAP product and the requirements for the mixing plant were also considered for high level of RAP addition. The primary objective was to produce HMA containing up to 20-50% RAP with a performance equivalent to the virgin HMA, i.e. manufactured without RAP. The level of RAP added to the mix depends on many variables and input parameters, however, within the framework of this paper these details, such as binder blend design and mix design will not be discussed.

This paper focuses on the performance tests carried out on laboratory and plant mixed asphalt mixes with varying levels of RAP and various based binders and the overall full depth asphalt (FDA) pavement performance was predicted through general mechanistic pavement design.

Transitioning from basic and empirical material properties through laboratory evaluation of asphalt mixes to long-term and reliable field performance prediction is the primary objective of pavement design and modelling.

II. PAVEMENT DESIGN TO CONSIDER PERFORMANCE DIFFERENCE – EMPIRICAL AND MECHANISTIC METHODS

Hungary, as a member of the European Union (EU) and the Comité Européen de Normalisation (CEN) - European Committee for Standardization – implements the EN standards on the national level. However, these standards only apply to road construction materials and test methods, and the EU and CEN do not provide harmonised standards for pavement design purposes. The current Hungarian approach in pavement structural design is semi-empirical (mechanistic-empirical).

The selection of input parameters into mechanistic-empirical design is crucial. This approach enables the introduction of innovative materials and technologies, and provides effective pavement structure build-ups. However, the mechanistic-empirical design can only address the structural capacity of the pavement structure and other aspects, such as the plastic deformation or low temperature behaviour also needs to be addressed through other means [5]. The determination of the structural capacity of new or existing pavement structures is one of the most interesting, but most difficult tasks of pavement engineering [6].

Reliable calculation of the allowable loading of a pavement structure considered extremely beneficial from the asset maintenance perspective as it allows allocation of resources and funding in a controlled

way and enables maintaining the level of service of the road [7].

The general mechanistic procedure (GMP) is limited to the assessment of load associated distresses and can be used for the assessment of new or existing pavement structures. The method uses computer software to determine the load induced critical strain responses in pavement layers. The critical responses assessed for asphalt materials is the horizontal tensile strain at the bottom of the layer and for subgrade and selected subgrade material it is the vertical compressive strain at the top of the layer [8].

The GMP requires the design moduli for existing pavement layers and the subgrade to be estimated as accurately as possible, for example by back-calculation [9]. This approach has been proven reliable and takes the uncertainties of the pavement design properties into consideration. Currently the Hungarian pavement overlay design method [10] utilises a mechanistic-empirical pavement design system, where a two layered pavement structure is transformed into an equivalent infinite layer using the deflection of the existing pavement structure as primary input and calculates allowable deflection using the general mechanistic procedure (GMP) approach [11, 12]. The method has its constraints, but basically provides a rational tool for pavement engineers. The method provides a solution solely for the asphalt overlay design with limited variability in material performance and unbound granular or concrete overlay is out of the scope for this method.

Originally the calculation of the tolerable deflection was based on the American Association of State Highway and Transportation Officials (AASHTO) investigation. Developments in the 1970s indicated that significantly variable pavement structures (unbound granular, full depth asphalt and semi-rigid) have very different tolerable deflections [13]. Based on further data collection and developments in September 1971 the Guidelines for the design of flexible pavement structures (159.215/1971 KPM) were issued (Hungarian abbreviation 'HUMU'), which had been used for more than 20 years after its first publication. By the end of the 1980s the shortcomings of this design method became obvious and, in line with international trends, the decision was made to utilise the pavement technology and testing advancements along with computer supported design and move towards the GMP. After several years of preparation, data collection, training and widespread technical discussions, the new Hungarian pavement design standard was issued for typical pavement structures; this was established in May 1992 and the method was introduced as a legislative requirement in 1994 as 'Dimensioning of asphalt pavements and their overlay' which is still valid today and only minor

modifications were made in the last three decades [14].

Unfortunately, significant advancement has not been made in the field of updating this design guideline since its first issue in the early 1990s, therefore the design inputs and methodology are now heavily outdated and cannot be kept up to date to incorporate developments in pavement materials technology. For that reason the benefits of any new pavement materials cannot be shown through a closed loop design as incorporating improved material properties and their transfer functions into the field performance prediction is simply not possible through this existing system. As a result the result of research and development activities cannot be incorporated and their positive life cycle cost benefit cannot be realised. This leads to wasting resources and energy and works against current worldwide trends towards building sustainable transport infrastructures.

Some research and development activity had been carried out in the last decade in order to fill this gap [15], however, no wide spread training and implementation was adopted by the road agencies and asset owners and these developments are significantly under-utilised despite their obvious benefits to the transport sector. There is an international move towards designing asphalt pavements that will last for an indefinite length of time. This concept is known as long life pavement, or perpetual pavement. Improved procedures have been developed for the design of longer life asphalt pavements in a cost effective manner by developing improved procedures for determining asphalt resilience and fatigue performance characterisation. Such approach utilises the flexural modulus master curves of asphalt mixes and makes it possible to reliably determine the design modulus of an asphalt material for any combination of load duration and temperature. It also becomes possible to develop mix specific fatigue models which enables a more direct comparison of mix designs based on expected field performance [16]. This approach requires extensive testing of asphalt mixes at various temperatures and also requires measured or predicted asphalt pavement temperature distributions in various depths. There are other emerging technologies in civil engineering, such as digital image correlation method (DICM) to predict displacements in structures [17].

A number of other countries have introduced sophisticated temperature prediction models, for example the Mechanistic-Empirical Pavement Design Guide (MEPDG) in the US [18]. Interestingly temperature prediction is not required in Hungary as detailed and in-depth pavement temperature data was collected and published widely for the Hungarian climate [19, 20, 21].

In this paper the GMP approach was used, i.e. strains were calculated in the pavement structure and compared with allowable strain levels derived from laboratory fatigue testing conducted at a single temperature. It should be however noted that further refinement of the calculations through the GMP is possible by considering pavement temperature profiles; there is a trend worldwide to utilise such application with the expected benefit to provide more detailed prediction in asphalt pavement long term performance. However, such a calculation requires fatigue testing at multiple temperatures and strain levels and completing such a time consuming test regime was out of scope.

III. PAVEMENT MODELS

The primary objective of the pavement design is to compare the load induced stresses and strains with the capacity of the structure. For example, knowing the geometric dimensions and materials of a simple structure and the load is also known, the strains and stresses can be directly calculated in any cross-section. If the properties of the material is also known the so-called allowable strains and stresses can be established, that is the highest level of repeated strain or stress tolerated by the material before failure occurs. This is the design method for any building structures, bridges or pavement structures (Fig. 1).

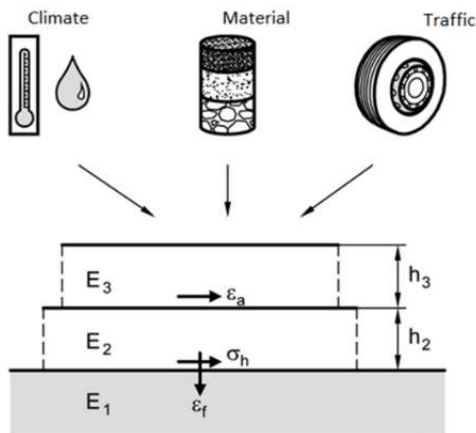


Figure 1. Simplified road pavement model

The mechanical behaviour of any layer within the pavement structure is described by the elastic or resilient modulus (E), Poisson's ratio (μ) and layer thickness (h). These three parameters provide the input into the mechanical model of the pavement structure. The load placed on top of the upper pavement layer induces strains, stresses and displacements in the structure and these can be calculated at any internal point of the multilayer system. Then the traffic volume and axle load is estimated and the allowable strains and stresses are determined from the fatigue properties of the relevant pavement layers. This is normally

established through advanced and detailed laboratory testing.

By comparing the actual and allowable strains and stresses, the design can be finalised. If the allowable strain or stress is higher than the actual strain or stress, the design is completed. Otherwise further iteration is required in the process, by either increasing the layer thickness(es) or selecting other material type and the new pavement structure has to undergo the above described process again up until the allowable strain or stress is higher than the actual strain or stress. Most design methods are also able to take into account the interlayer bond between layers, which is one of the most important requirements for the construction of a pavement structures. The interlayer bond significantly influences the actual strains and stresses within the pavement structure; this is not only a theoretical assumption, real life experience shows that pavement structures show premature failure if the bond between the asphalt layers is poor, for example due to paving on a dusty surface. Normally full bond is considered in between asphalt layers and slip (no bond) between the lowest asphalt layer and the underlying unbound granular base layer or subgrade.

IV. CALCULATING ACTUAL STRAINS AND STRESSES IN THE PAVEMENT MODEL

Moving forward only strains will be considered in this paper given that asphalt pavements are characterised by strain and not stress due to their visco-elastic nature. Complex and detailed calculations are now supported by powerful computer softwares such as (ALIZE, BISAR, WESLEA, ADtoPave, CIRCLY, etc.). Modern pavement design procedures calculate the following distress in the relevant layers:

- horizontal strain (ϵ_t) at the bottom of the lowest asphalt layer
- tensile stress (σ_t) at the bottom of hydraulically bound layer
- vertical compressive displacement (ϵ_v) at the top of the unbound granular base layer or the subgrade.

V. ALLOWABLE STRAINS

The fatigue properties of asphalt mixes can be determined by laboratory fatigue tests. The fatigue test provides the allowable strain versus loading cycles, which is a typical and so called Wöhler curve. From this fatigue function it can be estimated how many loading cycles the material can carry before any cracking develops. It should be noted that the fatigue functions derived from the laboratory tests are not transfer functions. Reliability factors should be utilised to relate a mean laboratory fatigue life to the in-service fatigue life at desired project reliability [22]. It should also be noted that high statistical

significance and data fit (R-squared) can be usually achieved by testing 18 specimens [23]. In this study maximum 12 beams were tested due to the large number of mixes and the associated long testing time. **Fig. 2**, **Fig. 3** and **Fig. 4** summarise the fatigue test results, where each point represents a single beam tested, and also provides the earlier mentioned fatigue curve. The allowable strains can be interpolated at 1 million cycles from each curve using regression analysis; the values for the asphalt mixes considered for pavement design are provided in **Table 2**, **Table 3** and **Table 4**.



Figure 2. Fatigue curves of AC22 binder (N) asphalt mix manufactured with plain binder and various RAP contents



Figure 3. Fatigue curves of AC22 binder (F) asphalt mix manufactured with plain binder and various RAP contents

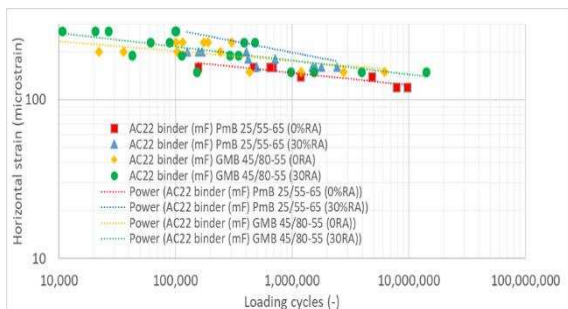


Figure 4. Fatigue curves of AC22 binder (mF) asphalt mix manufactured with polymer modified and crumb rubber modified binders and various RAP contents

VI. PAVEMENT MODELS AND ACTUAL STRAINS IN VARIOUS PAVEMENT MODELS

By utilising the principles of the GMP it becomes possible to compare the overall behaviour of various pavement structures built with various asphalt mixes. The primary objective of this paper was to provide performance comparison using asphalt mixes with various RAP contents and binder types.

The performance of different asphalt mixes within a pavement structure can be expressed in terms of allowable equivalent standard axle (ESA) repetition or required total asphalt thickness to meet set number of ESA (usually 1 million).

For the various pavement structures a single wearing course type was utilised. Asphalt wearing courses are functional layers and can be selected from a variety of asphalt types depending on the road type and traffic volume [24]. Since asphalt wearing courses have minimal contribution to the overall bearing capacity, the asphalt pavement and the objective of these calculations are to showcase the impact of various asphalt binder and base layer with varying RAP content, it was decided to model the wearing course by a 40mm thick, 4000 MPa layer without specifying its type. Also, only FDA pavement was considered, where the asphalt intermediate (binder), base and lower base layers were considered identical and their initial total thickness was 300 mm. The lower asphalt base layer is sitting on top of an infinite subgrade with uniform and minimum bearing capacity of 50 MPa. Poisson's ratio for all asphalt mixes was 0.35 and for the subgrade 0.45. For interlayer bond properties full bond was considered in between all asphalt layers and full slip between the lowest asphalt layer and the subgrade.

The main difference between the pavement structures were the various asphalt types with varying RAP content. Extensive laboratory testing provided the material parameters of these asphalt mixes and the variables were as follow:

- Virgin binder type – B (normal bitumen), PmB (polymer modified binder) and GmB (crumb rubber modified binder)
- RA content – varying from 0 to 50%
- Asphalt type – N (for normal traffic volume), F (for high traffic volume) and mF (for extremely high traffic volume)
- Laboratory and plant mixed asphalt mix.

For both laboratory and plant manufactured asphalt mixes RAP was sourced from Zsámbék depot of the Hungarian Main Roads. RAP was split into 0/11 and 11/22 fractions and their grading and binder contents were considered for laboratory batching and plant manufacturing to maintain target grading and binder content identical across all mixes. Softening point of the reclaimed binder was tested as

76°C and complex viscosity as 15 745 Pa.s at 60°C and 1 rad/s.

The first set of pavement structures consisted of an AC22 binder (N) asphalt layers, with varying RAP content. The benchmark mix was made with 0% RAP and the binder was B50/70 usually used for this asphalt mix. Two alternatives were made with 25% RAP and B70/100 binder, considering that the binder blend would provide a binder equivalent to the virgin B50/70, while the other version of mix was made with B50/70 virgin binder and 40% RAP. It was expected that the binder blend in the latter mix will be fairly viscous, more viscous than the benchmark B50/70 binder given that 40% RAP is added. The assumption was true given the modulus value of this asphalt mix exceeded the benchmark mix. The binder blend in the 25% RAP mix with B70/100 binder delivered modulus value comparable to the benchmark mix and it was considered that the binder blend design met its objectives.

With increasing stiffness, the fatigue property is expected to decrease in theory; the test results provided different outcome though. At 1 million load cycles, 131 microstrain was obtained for the 40% RAP mix with B50/70 binder compared to 101 microstrain for the benchmark mix. While this is theoretically not expected, in practice high RAP asphalt mixes tend to show better properties in terms of wheel tracking or moisture sensitivity. This is explained by the composition, i.e. very high proportion of ‘pre-coated’ aggregates are added through the addition of RAP [25]. For this reason the test results were considered valid and adopted for the calculations (**Table 2**). For all pavement structures analysed in this paper the modulus is characterised by tested resilient modulus value as determined according to EN 12697-26, indirect tensile test on cylindrical samples (IT-CY) [26].

Table 2. Pavement structures with AC22 binder (N) asphalt mix manufactured with plain binder and various RAP contents, laboratory mixed asphalt

Structural asphalt	AC22 binder (N)		
RA content	0%	25%	40%
Virgin binder type	50/70	70/100	50/70
Modulus (MPa)	6 600	7 200	10 400
Allowable strain (μs)	101	127	131
Subgrade (MPa)	50		

For the next set of pavement structures an AC22 binder (F) asphalt mix was considered; however, the performance properties were established from test results conducted on bulk samples obtained from large scale plant manufacturing process. The asphalt

mix was manufactured with RAP contents of 30-40-50% while the virgin binder was maintained as B70/100. As expected, the modulus value increased with the addition of more RAP as the binder blend

Table 3. Pavement structures with AC22 binder (F) asphalt mix manufactured with plain binder and various RAP contents, plant mixed asphalt

Structural asphalt	AC22 binder (F)		
RA content	30%	40%	50%
Virgin binder type	70/100	70/100	70/100
Modulus (MPa)	12 700	14 700	15 900
Allowable strain (μs)	122	121	131
Subgrade (MPa)	50		

became increasingly viscous. Similarly to the test properties showed in **Table 2**, better fatigue results were obtained for the 50% RAP mix when compared to the 30% RAP mix despite the binder blend was more viscous which also transpired in the modulus results. The reasons behind this observations are discussed above and the pavement inputs are summarised in **Table 3**.

For the last set of pavement structures an AC22 binder (mF) asphalt mix was considered with PmB and GmB binders. Both mixes were tested with 0% RAP for benchmarking and with the addition of 30% RAP. It was expected that when adding 30% RAP the original PmB and GmB properties cannot be maintained as the binder blend is heavily influenced by the RAP binder and the PmB and GmB properties are somehow ‘diluted’ (**Table 4**).

Asphalt mixes within the type (N, F and mF) were mixed or manufactured in a manner that combined aggregate grading, binder content and volumetric properties were targeted to be identical in order to close out the impact of volumetric variables. Binder blends were designed using sophisticated and controlled methods, however, these details are

Table 4. Pavement structures with AC22 binder (mF) asphalt mix manufactured with polymer modified and crumb rubber modified binder and various RAP contents, laboratory mixed asphalt

Structural asphalt	AC22 binder (mF)			
RA content	0%	30%	0%	30%
Virgin binder type	PmB 25/55-65		GmB 45/80-55	
Modulus (MPa)	6 300	7 200	5 500	7 400
Allowable strain (μs)	148	169	175	177
Subgrade (MPa)	50			

Table 5. Actual strain calculated at the bottom of the lower asphalt base layer

Asphalt layer	RA content (%)	Allowable strain (μs)	Actual strain (μs)
AC22 binder (N)	0	101	79
	25	127	73
	40	131	51
AC22 binder (F)	30	122	42
	40	121	37
	50	131	34
AC22 binder (mF)	0	148	82
	30	169	73
	0	175	93
	30	177	71

Table 6. Thickness requirement to meet allowable strain levels - pavement structures with equivalent bearing capacity

Asphalt layer	RA content (%)	Thickness at 1 million cycles (mm)	Thickness difference compared to benchmark (mm)
AC22 binder (N)	0	260	0
	25	220	40
	40	180	80
AC22 binder (F)	30	165	0
	40	170	-5
	50	160	5
AC22 binder (mF)	0	220	0
	30	190	30
	0	210	0
	30	180	30

discussed elsewhere [27, 28]. The actual strains within the relevant pavement structure were calculated using the WESLEA software and summarised in **Table 5**.

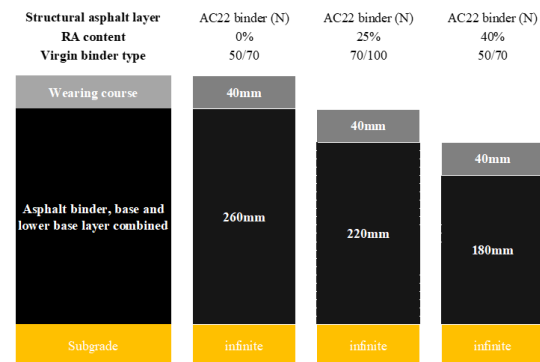
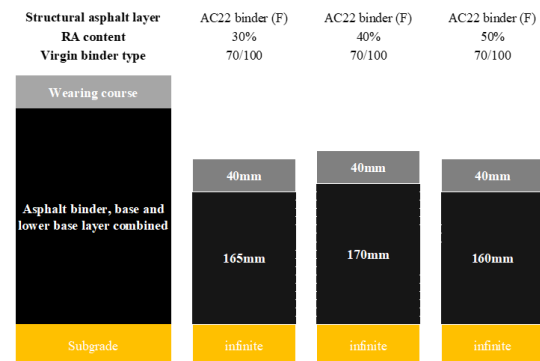
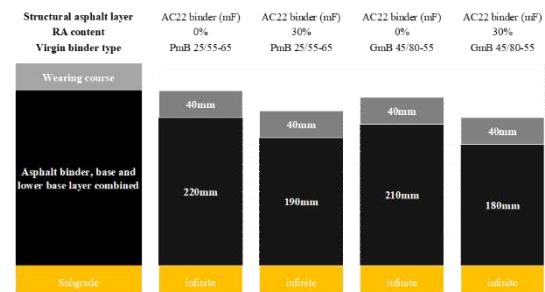
As per the design methodology the actual strain should be less than the allowable strain as expressed by equation (1), where $\varepsilon_t(N)$ is interpolated from the laboratory fatigue curve at 1 million ESA, as explained earlier.

$$\varepsilon_t \leq \varepsilon_t(N) \quad (1)$$

Based on the calculations, all pavement structures met the design criteria as the allowable strain was higher than the actual strain. All of these pavement structures could be utilised as they would be performing till the end of their design life. While these asphalt mixes have vastly different performance properties, they would be all considered equivalent in the currently adopted pavement design system.

In order to showcase the performance difference in between the various pavement structures and also

highlight the benefits of the GMP, the thickness of the combined structural asphalt layers was varied until the actual strain was equal to the allowable strain. In this case all pavement structures were identical in terms of their structural capacity. In **Table 6** the thicknesses are summarised along with the thickness differences compared to the pavement structures with baseline (benchmark) mixes; these are highlighted in grey. For a better overview **Fig. 5**, **Fig. 6** and **Fig. 7** visualise the outcomes of these calculations.

**Figure 5.** Summary of total binder, base and lower base asphalt layer thickness for pavement structures with AC22 binder (N) asphalt mix and equivalent bearing capacity**Figure 6.** Summary of total binder, base and lower base asphalt layer thickness for pavement structures with AC22 binder (F) asphalt mix and equivalent bearing capacity**Figure 7.** Summary of total binder, base and lower base asphalt layer thickness for pavement structures with AC22 binder (mF) asphalt mix and equivalent bearing capacity

VII. CONCLUSIONS

Considering a cost-benefit approach using the performance assessment of full depth asphalt pavements with high RAP content, there is an economic and in-situ performance benefit. Further positive impact can be achieved by the addition of warm mix additives, which positively impacts the performance and the carbon footprint due to lower production temperatures [29]. The benefits can be realised on high volume roads, such as motorway, due to their high material volume requirements. The associated risk with using high RAP content asphalt mixes, as shown in this paper, is not different to the application of virgin mixes, i.e. mixes manufactured without RAP. Incorporating high RAP content into low volume roads, such as residential streets certainly brings an economic benefit and the associated performance risk is even lower considering the lower traffic volume. The binder blend design is however critical for both high and low volume roads. The latter tends to deteriorate due to environmental loading and not traffic loading. For example over-stiffening a mix with the addition of high RAP and not carefully adjusting the binder blend in the mix by the appropriate selection of the virgin binder may lead to premature distress of the asphalt pavement due to diurnal temperature variations and associated thermal cracking.

The outcomes of this paper disproved the common perception that is high RAP content asphalt mix show substandard performance. The analysis performed in this paper found that asphalt mixes with high RAP content have high performance and present low risk for in-situ conditions, subject to correct mix design methodology, including binder blend characterisation, appropriate RAP

management and suitable asphalt plant capability for mass production.

The incorporation of high RAP content asphalt mixes into pavement structures results in responsible utilisation of resources and energy and lines up with worldwide trends towards building sustainable transport infrastructures.

ACKNOWLEDGEMENT

The research work outlined in this paper was completed as part of project 2020-1.1.2-PIACI-KFI-2020-00060, supported by the National Research, Development and Innovation Office of the Ministry of Innovation and Technology - National Research, Development and Innovation Fund.

AUTHOR CONTRIBUTIONS

Cs. Toth: Conceptualization, laboratory testing, review.

L. Petho: Mix design, analysis, writing and editing.

Sz. Rosta: Production control, testing and analysis.

P. Primusz: Pavement modelling.

DISCLOSURE STATEMENT

The authors have no known conflict of interest to declare.

ORCID

Cs. Toth <https://orcid.org/0000-0001-5065-5177>

P. Primusz <https://orcid.org/0000-0002-5966-6734>

REFERENCES

- [1] U. Zander, *Forschungsausrichtung in Balance von Ökologie und Ökonomie*, March 2022, Betonstraßentagung 2021, Bochum, Germany (in German).
- [2] *Asphalt in Figures, Asphalt in Figures – Provisional Figures 2021*, European Asphalt Pavement Association, Brussels – Belgium.
- [3] National Asphalt Pavement Association, *Asphalt Pavement Industry Survey on Recycled Materials and Warm-Mix Asphalt Usage: 2021*, Information Series 138, December 2022, United States.
- [4] National Asphalt Pavement Association, *High RAP Asphalt Pavements: Japan Practice – Lessons Learned*, Information Series 139, December 2015, United States.
- [5] L. Petho, Cs. Toth, *The development of pavement rehabilitation design guidelines for increasing the allowable axle load from 100 kN to 115 kN*, Proceedings of the 12th International Conference on Asphalt Pavements, pp.1577-1586, June 1-5, 2014, Raleigh, North Carolina, USA (ISBN: 978-1-138-02693-3).
- [6] L. Petho, Cs. Toth, 2012 Long-term pavement performance evaluation, 7th RILEM international conference on cracking in pavements, 20-22 June 2012, Delft, The Netherlands, Springer, pp. 267-277. https://doi.org/10.1007/978-94-007-4566-7_26
- [7] Austroads 2003, *Remaining Life of Road Infrastructure Assets: An Overview*, by P Robinson, B Clayton, A Alderson, K Sharp, AP-R235/03, Austroads, Sydney, NSW.
- [8] A.I.M. Claessen, J.M. Edwards et al., *Asphalt Pavement Design – The Shell Method*, International Conference on the Structural Design of Asphalt Pavements, Ann Arbor, 1977.

- [9] Austroads 2009, Guide to pavement technology: part 5: pavement evaluation and treatment design, by GW Jameson & M Shackleton, AGPT05/09, Austroads, Sydney, NSW.
- [10] Hungarian Road Society 2005, Design of road pavement structures and overlay design with asphalt surfacings, ÚT 2-1.202:2005, e-UT 06.03.13, Hungarian Road Society, Budapest, Hungary, (in Hungarian).
- [11] N. Odemark, 1949, Investigations as to the elastic properties of soils and design of pavements according to the theory of elasticity, meddlane 77, Statens Vaginstitut; Stockholm, Sweden.
- [12] E. Nemesdy, 1986, 'Calculation of the deflection and strains in multi-layers pavement structures', Review of Transportation Sciences, May 1986, pp. 193-201 (in Hungarian).
- [13] T. Boromisza, 1976, 'Bearing capacity of asphalt pavements based on deflection measurements', Revue of Roads and Civil Engineering, pp. 521–28 (in Hungarian).
- [14] P. Primusz, Cs. Toth, The benefits of designing fit-for purpose pavement structures, Aszfalt, XXVII, 2020/1 (in Hungarian).
- [15] P. Primusz, Cs. Toth, Simplified mechanistic design for asphalt pavements, Scientific Review of Transport, October 2018, (in Hungarian)
<https://doi.org/10.24228/KTSZ.2018.5.2>
- [16] E. Denneman, J. Lee, M. Dias, L. Petho, 2016, Improved design procedures for asphalt pavements, AP-R511-16, Austroads, Sydney, NSW (ISBN 978-1-925451-02-3).
- [17] Sz. Szalai, B. Eller et. al, Investigation of deformations of ballasted railway track during collapse using the Digital Image Correlation Method (DICM), Reports in Mechanical Engineering 3: 1 pp. 258-282. , 25 p. (2022)
<https://doi.org/10.31181/rme20016032022s>
- [18] Q. Li, D. X. Xiao, K. C. Wang, K. D. Hall and Y. Qiu, "Mechanistic-empirical pavement design guide (MEPDG): a bird's-eye view," Journal of Modern Transportation, vol. 19, no. 2, pp. 114-133, 2011.
- [19] S. Cho, Cs. Toth, L. Petho, Predicting asphalt pavement temperatures as an input for a mechanistic pavement design in Central-European climate, Eleventh International Conference on the Bearing Capacity of Roads, Railways and Airfields, Volume 1, CRC Press, 2021, London, UK.
- [20] Cs. Toth, L. Petho, Calculating the equivalent temperature for mechanistic pavement design according to the French method for Hungarian climatic conditions, Acta Technica Jaurinensis, Vol. 14, No. 3, pp.244-258, 2021.
<https://doi.org/10.14513/actatechjaur.00602>
- [21] L. Petho, 2008, 'Influence of temperature distribution on the design of pavement structures', Periodica Polytechnica. Civil Engineering, vol. 52, no.1, pp. 45-53.
<https://doi.org/10.3311/pp.ci.2008-1.07>
- [22] Austroads 2010, Guide to pavement technology: part 2: pavement structural design, by GW Jameson, AGPT02/10, Austroads, Sydney, NSW.
- [23] EN 12697-24, Bituminous mixtures. Test methods for hot mix asphalt. Part 24: Resistance to fatigue.
- [24] L. Gaspar, Zs. Bencze, Literature review on the selection of optimal wearing course types for heavy duty pavements, Utugyi Lapok, 4/8/2016, ISSN: 2064-0919 (in Hungarian).
- [25] L. Petho, E. Denneman, 2016, Maximising the use of reclaimed asphalt pavement in asphalt mix design: field validation, AP-R517-16, Austroads, Sydney, NSW (ISBN 978-1-925451-09-2).
- [26] EN12697-26:2018, Bituminous mixtures - Test methods - Part 26: Stiffness.
- [27] Sz. Rosta, L. Gaspar, "Útépítési bitumen és visszanyert bitumen ele-gyének dinamikai viszkozitás számítása és előrebecslési lehetősége" (Dynamic viscosity calculation and prediction possibilities for the blend of pavement grade bitumen and bitumen from recycled asphalt), Közlekedéstudományi Szemle, 73(1), pp. 21-38. (in Hungarian)
<https://doi.org/10.24228/KTSZ.2023.1.2>
- [28] Sz. Rosta, L. Gaspar, (2023), Dynamic viscosity prediction of blends of paving grade bitumen with reclaimed bitumen, Periodica Polytechnica Transportation Engineering 2023 (in press).
- [29] B. Sengoz, A. Topal, J. Oner, M. Yilmaz, P. Aghazadeh Dokandari, B. Kok, B. V. "Performance Evaluation of Warm Mix Asphalt Mixtures with Recycled Asphalt Pavement", Periodica Polytechnica Civil Engineering, 61(1), pp. 117–127, 2017.
<https://doi.org/10.3311/PPci.8498>



This article is an open access article distributed under the terms and conditions of the Creative Commons Attribution NonCommercial (CC BY-NC 4.0) license.

Investigation of the cutting force and surface profile error when free form milling

Bálint Varga^{1,*}, Balázs Mikó¹

¹ Institute of Materials- and Production Science, Óbuda University
Népszínház u. 8 1081 Budapest Hungary
*e-mail: varga.balint@bgk.uni-obuda.hu

Submitted: 18/01/2023 Accepted: 19/02/2023 Published online: 22/02/2023

Abstract: Machining free-form shaped surfaces is a widespread task. Aerospace, automotive, mould making and many other sectors are challenged by ever increasing demands for precision and economy. In ball-end milling, the constantly changing cutting conditions affect the shape and volume of the chip, as well as the tool load and the quality of the resulting surface. It is important to know the cutting force for a given surface characteristic, because this makes it easier to plan the machining process. The prediction of cutting forces is very important for optimising machining strategies and parameters to achieve the required accuracy. In the experiments, the forces on the tool and the surface geometric accuracy were measured by milling test surfaces of 42CrMo4 with different cutting parameters. Based on the measured values, the average cutting force was determined, the variance of the force variation was investigated and the force momentum, which takes into account the machining time. The aim of this paper is to investigate and compare the cutting force and the surface profile error of the resulting surface during finishing milling with a ball-end milling cutter.

Keywords: Free-form surface; Ball-end milling; Cutting force; Surface profile error

I. INTRODUCTION

Free-form surface milling is widely used in machine and tool manufacturing, foundry, aerospace, automotive. Their machining requires high productivity as well as high precision. There are many different aspects to be taken into account in the manufacturing process. The technological parameters of the cutting process, the tool parameters and the tool path must be defined. Productivity and accuracy must be planned within a given range of machining possibilities. Measurement options that can be used during the process should be considered to reduce the number of rejects. In addition, moulding tools are usually made of hard-to-machine alloy steels, which makes them even more difficult to produce [1][2].

The quality of the machined surface is determined by a number of parameters. The literature focuses primarily on surface roughness [3], but geometric accuracy is an equally important requirement in industry. Increasing demands are making it more and more difficult for industry to meet precision requirements. Accuracy is assessed on three criteria: (1) surface roughness, (2) geometric accuracy, (3) dimensional accuracy. Geometric tolerances defined

by standards [4] are becoming increasingly important in industry, so the collection of design, measurement and manufacturing knowledge related to them is an important task [5][6][7].

The specification and verification of geometrical tolerances is a complex task, which, in addition to the interpretation of standards, has to take into account the mathematical evaluation of geometrical tolerances [8] and the number and location of sampling points. Several methods have been investigated. Examples include the B-spline curve method, a method using a fuzzy system [9][10].

Parts with free-form surfaces are milled on computer numerically controlled (CNC) machine tools using a ball-end milling tool. To achieve sufficient accuracy and productivity, machining can be divided into three main parts: roughing, intermediate machining and finishing [11]. In the first two stages, most of the excess material is removed, while in the finishing stage only a uniform thickness of material remains to be removed. Finishing is the final machining operation to produce the final part surface. It can therefore be said that this machining stage has the greatest impact on the quality of the surface.

In ball-end milling, the nature of the free-form surface means that the machining conditions are constantly changing. As well as the size of the workpiece constantly changing, the working edge length may also be constantly varying. It can be said that the machining conditions are a constantly changing system, which affects the shape and size of the chip and the cutting force.

In machining analysis, it is essential to have as accurate as possible knowledge of the cutter-workpiece engagement (CWE) [12]. CWE can be divided into three types: the first is the body modelling method based on Boolean operation [13], the second is the Z-map method based on discrete elements [14], and the third is the boundary method based on analytical or numerical calculations [15].

Machining force prediction models can help the designer to choose the right machining parameters. In machining design, CAM systems currently do not have data to predict the expected cutting forces.

This paper presents an investigation of the geometrical tolerances of free-form surfaces produced by ball-end milling and the forces involved in their manufacture.

II. METHODS AND EQUIPMENTS

In the tests, the envelope size of the test piece was 80x80x30mm with a cylindrical surface of 45mm radius. This section is joined to a 10 mm wide horizontal plane with a radius of 10 mm. A concave (CV) and a convex (CX) part were created to compare the nature of the surfaces. The height and depth of the cylindrical part are 9.2 mm (**Fig. 1**).

The material of the test parts was 42CrMo4 (1.7225; $R_m = 1000$ MPa), a low alloy steel, which is one of the low alloy steels containing chromium, molybdenum, manganese (**Table 1**). Toughness with high fatigue strength and good low temperature

impact resistance. 42CrMo4 alloy steel is widely used for engineering applications.

Table 1. Chemical content of the 42CrMo4 steel

C	Si	Mn	Mo	S	Cr	Ni
0.43	0.26	0.65	0.16	0.021	1.07	0.19

Machining was performed on a Mazak 410 A-II CNC machining centre. A Fraisa X7450.450 type milling tool with a diameter of 10 mm ($D_c=10$ mm) was used. The number of teeth was 4 ($z=4$). The tools were clamped with an EMUGE-FRANKEN SK40 type cold clamping fixture (PowerGrip). During machining, the coolant was applied by the flooding method (Aquamet 40, 6-8% emulsion, yield about 30 l/min).

The CNC programs were produced using CATIA v5 CAD/CAM system. During the finishing operation, the ball-end mill followed the surface parallel to the plane of **Figure 1**.

Table 2. Cutting parameters

Part	f_z [mm]	a_e [mm]
1	0.08	0.35
2	0.08	0.25
3	0.16	0.15
4	0.12	0.15
5	0.08	0.15
6	0.16	0.35

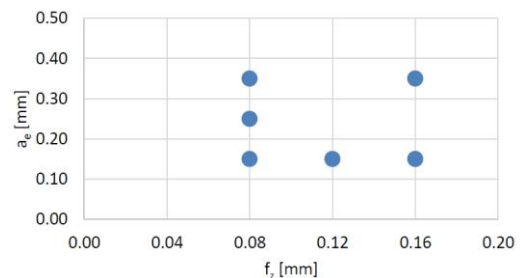


Figure 2. Sets of feed per tooth and width of cut

The spindle speed was 5100 rpm, which means a nominal cutting speed of 160 m/min. The depth of cut was $a_p = 0.3$ mm, which was ensured by pre-finishing. The feed and width of cut were varied in 3-3 levels as shown in **Table 2** and **Fig. 2**.

The milling times for a toolpath and the machining times for a surface are shown in **Fig. 3**. For a single toolpath, the feed per tooth determines the time, but for the whole surface, the width of cut has an effect.

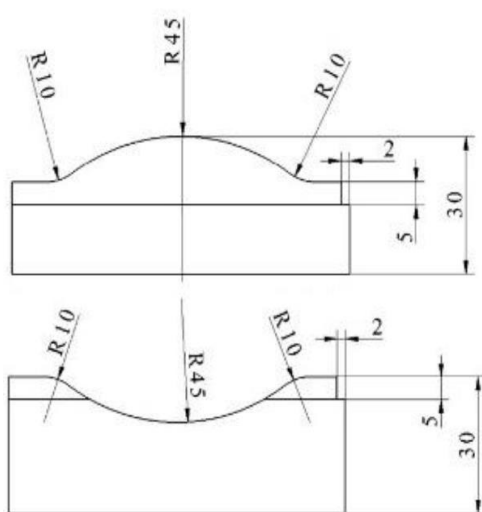


Figure 1. Geometry of the test surfaces

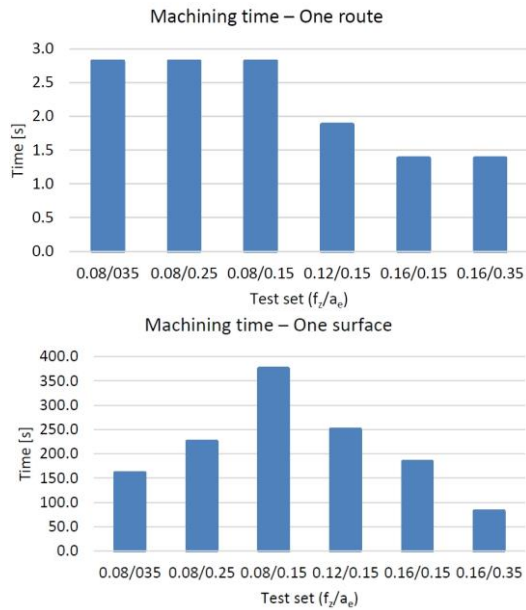


Figure 3. Machining time

The cutting forces were measured using a KISTLER 5019 3-component force measuring device. The data were evaluated by the software DynoWare. The force measurements were performed at a frequency of 2000 Hz, in the down milling (D) and upmilling (U) phase. The measured values were corrected for zero offset.

As shown in Fig. 4, the periodical nature of the milling process and the continuous variation in milling conditions cause the force measurement values to fluctuate significantly. For processability, filtering was applied: the average values of 25

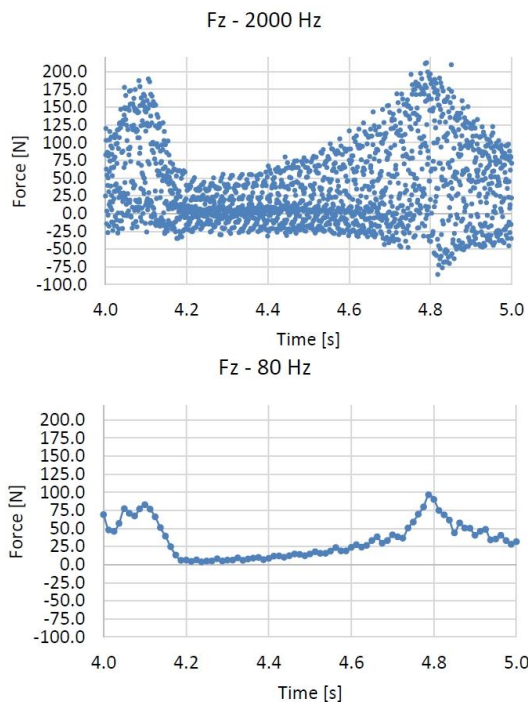


Figure 4. Measured and filtered F_z force component (example)

measurements were used for the evaluation. This results in a measurement frequency of 80 Hz. It means 80 points, instead of 2000 during 1 second. The effect of this is shown in Fig. 4 in case of a 1-second long data series of the axial direction (F_z) force component of the convex test piece No.6 ($f_z = 0.16$; $a_e = 0.35$).

The resultant force was calculated as the vector sum of the force components.

The surface profile tolerance is the tolerance field formed by symmetrically offsetting, which has 3 degrees of freedom (Fig. 5). The measured points must be located in this volume. The tolerance can be adjusted by reducing the number of degrees of freedom of the tolerance field by specifying datum.

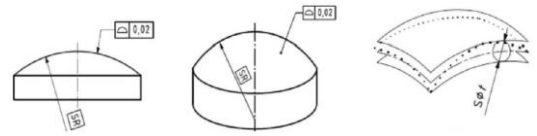


Figure 5. Surface profile tolerance

Points on the surface were measured using a Mitutoyo Crysta-Plus 544 coordinate measuring machine with a 3 mm nominal diameter probe, a Renishaw TP20 touch-trigger probe. 105 points were measured on the surface along a 5x21 grid. The geometric error was evaluated based on the measured points using Evolve Smart Profile v6 software (Fig. 6), which is capable of comparing the

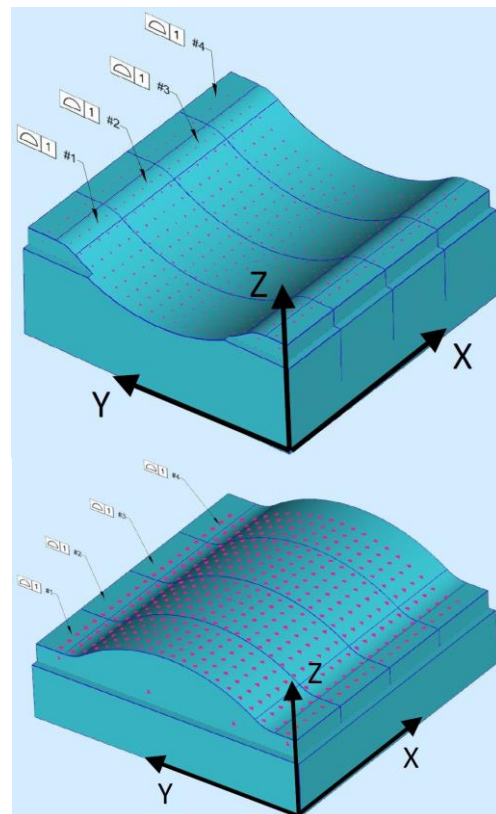


Figure 6. Point cloud on the surface

measured points to a theoretical CAD model of the part under test based on a point cloud recorded by any measurement system.

III. RESULTS

The character of the time variation of the forces during milling is described for setting No.1 ($f_z=0.08$; $a_e=0.35$). The nature of each component is similar for all settings.

Since the cutting is in the y direction, F_x , the force component in the x direction, is the passive force. F_y , the y direction component, is the force in the feed direction, and F_z , the z direction component, is the axial force in the tool axis direction. The coordinate system is indicated in the **Fig. 6**. The sum of the three

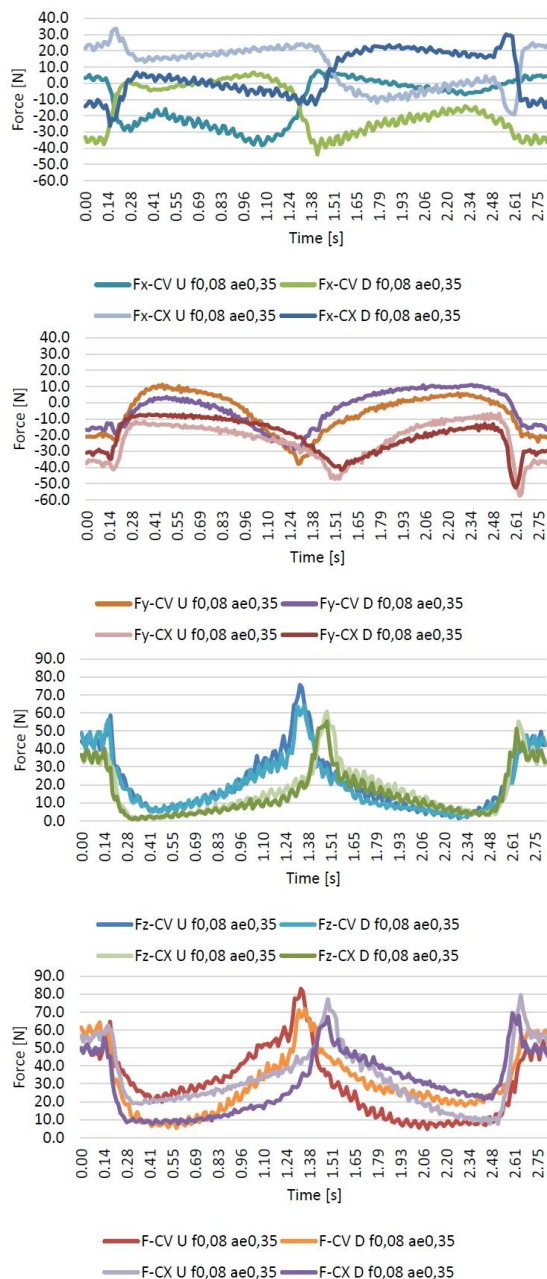


Figure 7. Cutting forces

force component vectors is the resultant cutting force (F). The diagrams show the variation of the forces over time for a single toolpath (**Fig. 7**).

For each of these diagrams, the effect of the change in the surface area is clearly visible. The character of the force changes at the inflection point of the surfaces. The direction of the force changes for passive force (F_x), and the diagrams are nearly symmetrical for upcut (U, $y+$ direction feed) and downcut (D, $y-$ direction feed) cases. The force F_x fluctuates around 0 in some sections.

For the force in the feed direction (F_y), there is an extreme value of the force at the straight section, and then also near the inflection point. For axial forces (F_z), the character is similar but the variation is larger. For all three force components, a rapid decrease in force is observed as the force leaves the horizontal section, followed by a slow increase as the force approaches the inflection point. For the concave (CV) surface the maximum is just before the inflection point, for the convex (CX) surface the force maximum is slightly after.

The nature and magnitude of the resultant cutting force is determined by the axial force. The average values of the resultant forces are shown in **Fig. 8**. As can be seen, the differences are small in the case of up- and down milling, and for concave and convex surfaces. The feed rate and width of cut have a greater effect on the cutting force. The diagram also shows that the width of cut has a greater effect on the resultant force than the feed. The largest value is of course at the maximum parameters tested.

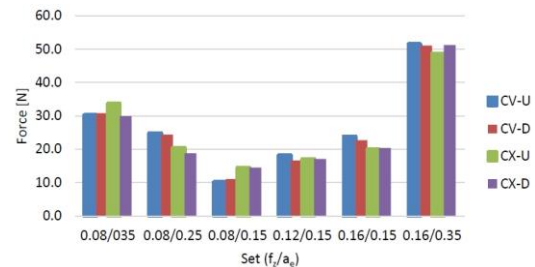


Figure 8. Average cutting force

The variation in the value of the force along a path can be described by the standard deviation. As shown in **Figure 9**, it follows the trends observed for the force. The relative value of the standard deviation

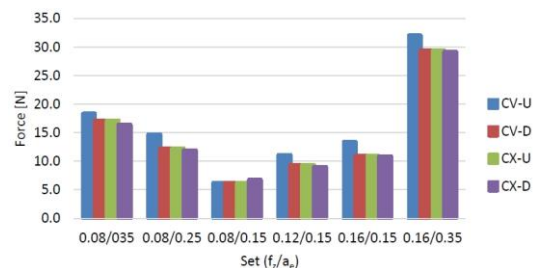


Figure 9. Standard deviation of the cutting force

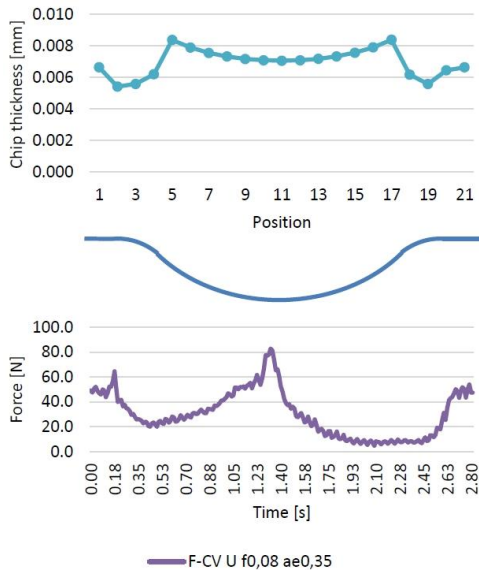


Figure 10. Chip thickness and cutting force (CV; $f_z=0.08$; $a_e=0.35$)

is 43-62%, indicating that there is a significant variation of the force along the toolpath.

The volume and average thickness of the uncut chips along the milling path were determined using CAD modelling [16]. The values for setting No.1 are shown in **Fig. 10** and **Fig. 11**. Comparing the change in surface area, the change in chip thickness and the change in cutting force, it can be concluded that the force value is not only affected by the chip thickness, as the increase in force in the middle part of the surface is not explained by the change in chip thickness.

The increase in force is due to changes in the machining conditions. The tip (cross edge) of the

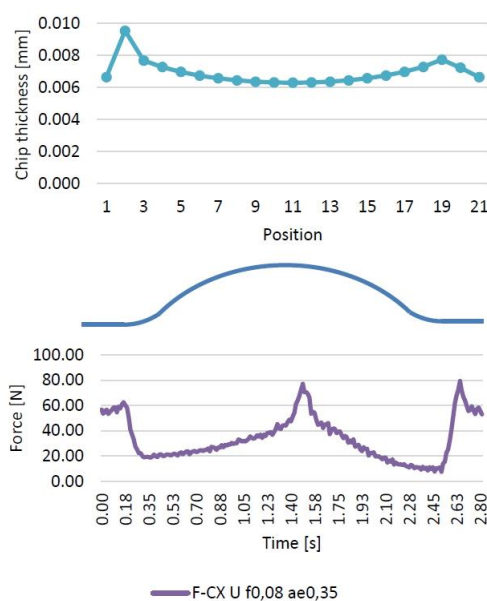


Figure 11. Chip thickness and cutting force (CX; $f_z=0.08$; $a_e=0.35$)

tool is also at work on the surface sections close to the horizontal. However, here the cutting speed is close to 0 due to the small diameter and the chip separation is limited due to the edge design. Consequently, as the chips separate, the elastic and plastic deformation of the material increases, which is reflected in an increase in the force acting on the tool.

Machining times vary for each setting (**Fig. 3**). The effect is shown by the force momentum, which is actually the area under the force-time function. The force momentum is a suitable tool for comparing force values measured under varying machining conditions.

The force momentum value takes into account both the magnitude and variation of the force and the duration of the machining operation. **Fig. 12** shows the values for a toolpath. As the feed rate is reduced (setting No.1-2-5), the value decreases. Then, the increase in force caused by increasing the width of cut (setting No.5-4-3) is compensated by a shorter milling time. In the last setting with maximum values (No.6), the high force values are compensated by the very short milling time, so that the force momentum value is lower than in the case of setting No.1.

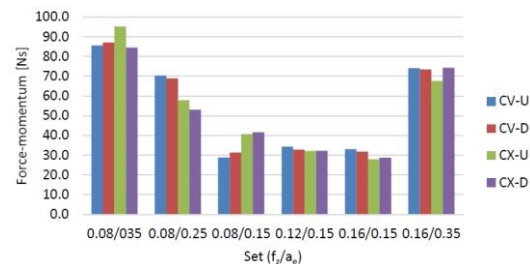


Figure 12. Force momentum for one tool path

Calculating the force momentum value for the entire surface, the upmilling and downmilling path sections must be considered simultaneously. The values (**Fig. 13**) are higher for the No.1 setting. For settings No.2 and No.5, the values determined for the concave and convex surfaces are significantly different. For settings 5-3-4-6, essentially identical values are obtained.

The surface profile error of each surface is shown in **Fig. 14**, ranging from 0.06 mm to 0.14 mm. As

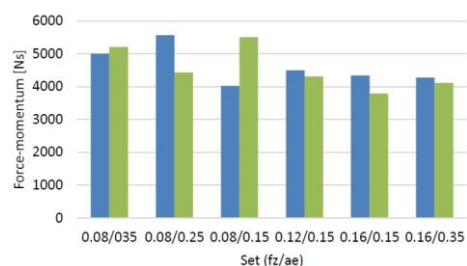


Figure 13. Force momentum on the surface

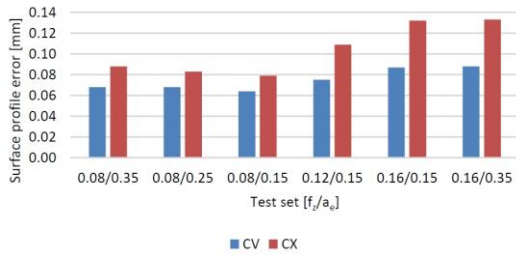


Figure 14. Surface profile error

can be seen, the error of the convex surfaces is larger, even though no large difference in the average values of the resultant force was observed. While for the cutting forces, the width of cut shows a larger effect, the geometric error increased to a larger scale with increasing feed rate and the width of cut has minimal effect. This may be due to the different change of the force components along the toolpath, which requires further investigation.

The surface profile error indicates the thickness of a defect band, but the deviation varies along the surface. **Fig. 15** and **Fig. 16** show the deviation within the surface profile tolerance for surfaces with setting No.1. These deviations follow well the evolution of the cutting force. At the horizontal start and end sections and at the centre of the surface, where the maximum value of the force was measured (**Fig. 7**), the surface deviation is the largest in the positive direction. At the through radius, where the force decreases, the surface shows a large negative deviation.

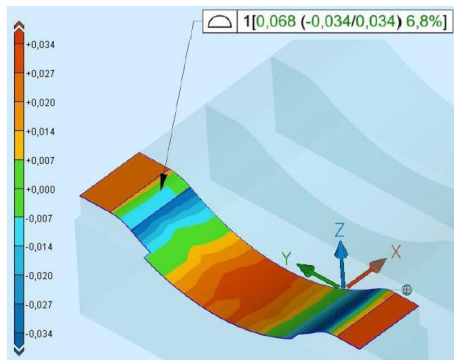


Figure 15. Surface profile error map
(CV; $f_z=0.08$; $a_e=0.35$)

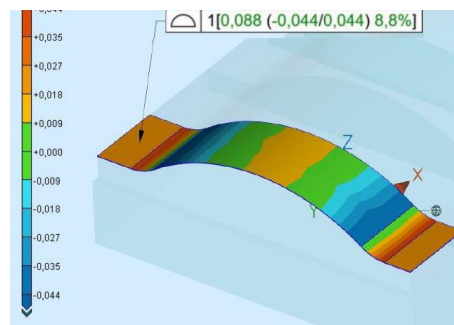


Figure 16. Surface profile error map
(CX; $f_z=0.08$; $a_e=0.35$)

IV. CONCLUSION

When machining free-form surfaces with ball-end milling, a CAM system must be used to create a toolpath that ensures dimensional and shape accuracy of the surface and the correct surface roughness. The combination of these requirements is only possible by selecting the right motion strategy, tool geometry and cutting parameters.

In the present study, the cutting forces and surface geometric accuracy of 42CrMo4 test parts were measured at different feed per tooth and width of cut (side step) parameters.

Based on the measurement data, it can be concluded that

- the cutting force varies greatly during the machining process;
- the geometric accuracy of the milled surface follows the change in cutting force, but the feed and the width of cut have different effect,
- the force momentum can be used to effectively compare the effect of changes in force and machining time caused by machining parameters;
- the change in force is determined not only by the change in the cross-section of the chip, but also by the conditions of the section of the tool that is actually working;
- when the tip of the tool is involved in the machining operation (surfaces close to horizontal), the cutting force increases significantly, the form deviation increases;

Based on the results obtained, it can be concluded that for the smooth milling of free-form surfaces with a spherical tool, a milling strategy should be chosen in which the tip of the tool is not involved in the machining process in order to reduce the cutting force and the shape deviation.

When determining the cutting force by calculation, the position of the working section of the tool must be taken into account in addition to the chip cross-section, as this also has a significant effect on the cutting force.

Further research could investigate the effect of tool design on cutting forces and deflection, for example for different numbers of teeth.

AUTHOR CONTRIBUTIONS

Varga B.: Conceptualization, Experiments, Force and chip analysis, Writing.

Mikó B.: GPS analysis, Writing, Review and editing, Supervision.

DISCLOSURE STATEMENT

The authors declare that they have no known competing financial interests or personal relationships that could have appeared to influence the work reported in this paper.

ORCID

Varga B: <http://orcid.org/0000-0002-0281-1996>

Mikó B. <http://orcid.org/0000-0003-3609-0290>

REFERENCES

- [1] Thakur, D.G., Ramamoorthy, B., Vijayaraghavan, L., Effect of cutting parameters on the degree of work hardening and tool life during high-speed machining of Inconel 718. *Int. J. Adv. Manuf. Technol.* 59 (2012) pp. 483–489. <https://doi.org/10.1007/s00170-011-3529-6>
- [2] Olufayo, O.A. et al., Machinability of Rene 65 Superalloy Materials 12 (2019) id:2034 <https://doi.org/10.3390/ma12122034>
- [3] Kundrák J., Felhő Cs., Nagy A., Analysis and prediction of roughness of face milled surfaces using CAD model. *Manufacturing Technology* 22 (5) (2022) pp.558-572. <https://doi.org/10.21062/mft.2022.061>
- [4] Geometrical Product Specifications (GPS) - Geometrical Tolerancing-Tolerances of Form, Orientation, Location and Run-Out; ISO 1101-2017 (2017).
- [5] Varga, J. et al., The Influence of Automated Machining Strategy on Geometric Deviations of Machined Surfaces. *Appl. Sci.* 11 (2021) id:2353.
- [6] Płowucha, W. et al., Geometrical product specification and verification as toolbox to meet up-to-date technical requirements. In *Proceedings of the 11th International Scientific Conference “Coordinate Measuring Technique” CMT2014, Bielsko-Biala 2014*, pp. 131–139.
- [7] Varga Gy., Dezső G., Szigeti F., Shape accuracy improvement in selective laser-melted Ti6Al4V cylindrical parts by sliding friction diamond burnishing, *Machines* 10 (10) id:949. <https://doi.org/10.3390/machines10100949>
- [8] Gosavi, A., Cudney, E.A., Form Errors in Precision Metrology: A Survey of Measurement Techniques. *Qual. Eng.* 24 (2012) pp. 369–380. <https://doi.org/10.1080/08982112.2011.652583>
- [9] Zhao, D. et al., Measurement point sampling method for inspection of parts with free-form surfaces. *Adv. Mech. Eng.* 10 (2018) pp. 1–12. <https://doi.org/10.1177/1687814018809577>
- [10] Magdzak, M., Chandima Ratnayake, R.M., Contact Coordinate Measurements of Free-Form Surfaces: A FIS for Optimal Distribution of Measurement Points. In *Proceedings of the 2018 IEEE International Conference on Industrial Engineering and Engineering Management (IEEM), Bangkok, 2018*. <https://doi.org/10.1109/IEEM.2018.8607476>
- [11] Kiswanto G., Hendriko H., Duc E., An analytical method for obtaining cutter workpiece engagement during a semi-finish in five-axis milling. *Comput Des* 55 (2014) pp. 81–93. <https://doi.org/10.1016/j.cad.2014.05.003>
- [12] Mou W.. et al., A Prediction Model of Cutting Force about Ball End Milling for Sculptured Surface, *Mathematical Problems in Engineering*; 2020, id: 1389718 <https://doi.org/10.1155/2020/1389718>
- [13] Larue A. and Altintas Y., Simulation of flank milling processes, *International Journal of Machine Tools and Manufacture*, 45(4-5) (2005) pp. 549–559.
- [14] Kim G. M., Cho P. J., and Chu C. N., Cutting force prediction of sculptured surface ball-end milling using Z-map, *International Journal of Machine Tools and Manufacture*, 40(2) (2000) pp 277–291.
- [15] Gupta S. K., et al., Geometric algorithms for computing cutter engagement functions in 2.5D milling operations, *Computer-Aided Design*, 37 (14) (2005) pp. 1469–1480.
- [16] Varga B., Mikó B., CAD modelling of the chip shape in case of ball-end milling. *Engineering and IT Solutions* (2) (2022) pp.30-38. <https://doi.org/10.37775/EIS.2022.2.3>



This article is an open access article distributed under the terms and conditions of the Creative Commons Attribution NonCommercial (CC BY-NC 4.0) license.